JNC TN9400 2000-005

02

分工

# SIMMER-Ⅲ Analytic Equation-of-State Model

May 1999

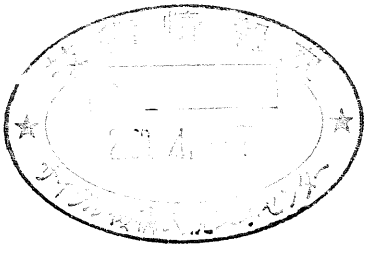

O-ARAI ENGINEERING CENTER

JAPAN NUCLEAR CYCLE DEVELOPMENT INSTITUTE

# SIMMER-III Analytic Equation-of-State Model

K. Morita * [a], Y. Tobita *, Sa. Kondo *
E. A. Fischer * [b], K. Thurnay **

## Abstract

An improved analytic equation-of-state (EOS) model using flexible thermodynamic functions is developed for a reactor safety analysis code, SIMMER-III. The present EOS model is designed to have adequate accuracy in describing thermodynamic properties of reactor-core materials over wide temperature and pressure ranges and to consistently satisfy basic thermodynamic relationships without deterioration of the computing efficiency. The fluid-dynamic algorithm for pressure iteration consistently coupled with the EOS model is also described in the present report. The EOS data of the basic core materials, uranium dioxide, mixed-oxide fuel, stainless steel, and sodium, are developed up to the critical point by compiling the most up-to-date and reliable sources using basic thermodynamic relationships. The thermodynamic consistency and accuracy of the evaluated EOS data are also discussed by comparison with the available sources.

---

* Fast Reactor Safety Engineering Group, Sodium and Safety Engineering Division
O-arai Engineering Center, JNC

** Forschungszentrum Karlsruhe, Institut für Neutronenphysik und Reaktortechnik, Germany

a Present affiliation: Institute of Environmental Systems, Kyusyu University

b International Fellow
Present affiliation: Forschungszentrum Karlsruhe
Institut für Neutronenphysik und Reaktortechnik, Germany

JNC TN9400 2000 − 005
May, 1999

# SIMMER-III 解析的状態方程式モデル (研究報告書)

守田　幸路 *[a], 飛田　吉春 *, 近藤　悟 *
E. A. Fischer *[b], K. Thurnay **

## 要　旨

高速炉安全解析コード SIMMER-III で使用する解析的状態方程式（EOS）モデルを開発した。汎用的な熱力学的関数式を使用した本モデルは、計算効率を犠牲にすることなく、幅広い温度および圧力領域での炉心物質の熱力学的特性を充分な精度で記述し、基本的な熱力学的関係を満足するように設計されている。本報告書では、この EOS モデルと結合した圧力反復計算の流体力学アルゴリズムについても記述した。二酸化ウラン、混合酸化物燃料、ステンレス鋼およびナトリウムの臨界点までの EOS データについては、最新でかつ最も信頼できるデータに基づき、基本的な熱力学的関係を用いて求めた。EOS データの熱力学的整合性と精度についても既存データと比較することで議論した。

---

*　大洗工学センター，ナトリウム・安全工学試験部，高速炉安全工学グループ
**　独国カールスルーエ研究所
a　現所属　九州大学工学部付属　環境システム科学研究センター
b　国際特別研究員，現所属　独国カールスルーエ研究所

# Contents

## List of tables

## List of figures

## Chapter 1. Introduction

To analyze postulated severe-accident sequence in liquid-metal fast reactors (LMFRs), we need thermodynamic properties of reactor-core materials over very wide ranges of temperature and pressure. Especially, for an accident analysis code like SIMMER-III (Kondo et al., 1992), which was developed to simulate multi-phase, multi-component thermal-hydraulic phenomena occurring during accident progression, the properties up to the critical point are required to complete an equation-of-state (EOS) model. In general, EOSs are the thermodynamic relationships among independent state variables constituting the basic fluid-dynamics equations and hence the EOS model is required to close and complete them. Moreover it is crucial from the viewpoints of numerical accuracy and stability, as well as computing efficiency in multi-phase, multi-component flow codes. Neither of the previous codes SIMMER-II (Bohl and Luck, 1990) nor AFDM (Bohl et al., 1990) was satisfactory from these aspects. In SIMMER–II, inconsistencies in the simple analytic EOS introduced difficulty in determining vapor temperature at high pressure, resulting in many numerical problems. To resolve these problems, a use of a tabular EOS model (Henneges and Kleinheins, 1994) was tried in AFDM, but was not successful due to the combined effects of time–consuming table search/interpolation and the iteration to obtain mechanical equilibrium.

Based on the past experiences, therefore, an improved analytic EOS model using flexible thermodynamic functions is newly developed to treat the basic reactor-core materials including mixed-oxide fuel, steel, sodium, control ($B_4C$) and fission gas for the SIMMER-III code. This model assumes the immiscibility of the reactor-core materials, such that a unique EOS can be defined for each material. Proposed functions are formulated so as to have adequate accuracy in thermodynamic properties of the reactor-core materials at high temperature and high pressure, and to consistently satisfy basic thermodynamic relationships over the wide temperature range from the solid to supercritical state. The function forms use polynomial equations for the liquid and solid phases and a modified Redlich-Kwong (MRK) equation for the vapor phase (Fischer, 1992). The latter equation is almost as simple as the well-known van der Waals equation, but it is much more accurate at least for vapors. Moreover, the MRK equation is newly extended to include the dimerization process of sodium vapor so as to describe the properties of sodium vapor appropriately. The heat- and mass-transfer model (Morita et al., 1994) requires additional thermodynamic properties and their derivatives to evaluate heat- and mass-transfer rates at each binary contact interface of different energy components. The present analytic EOS model also defines the saturation temperature, specific volumes, internal energies, and the heats of vaporization, based on the vapor partial pressure.

In this report, we describe the analytic EOS model for use in SIMMER-III and thermodynamic relationships among state variables, which are also necessary for evaluation of thermodynamic properties from available sources. In Appendix A we go into details about the

MRK equation extended to a reacting system. The EOS modeling is also a very important concern in designing the fluid-dynamics algorithm for pressure iteration and so a newly introduced scheme to SIMMER-III pressure iteration is described. All constants in the proposed EOS functions for the basic reactor-core materials can be found in Chapter 4.

## Chapter 2. Analytic EOS model

### *2.1. EOS functions for solid properties*

The EOS relationships are given for the structure components and solid particles in the liquid fields. Structure components, such as can wall, cladding, pin fuel and crust fuel, are assumed to be incompressible with polynomial fits for temperature, $T_{Sm}$, and specific volume, $v_{Sm}$, as a function of specific internal energy, $e_{Sm}$. The function for the structure temperature is given by

$$T_{Sm} = T_{Sol,M}[1 - a_{S1,M}(1-u_{Sm}) - a_{S2,M}(1-u_{Sm})^2 - a_{S3,M}(1-u_{Sm})^3],$$

$$e_{Sm} < e_{Sol,M}, \text{ and} \qquad (1a)$$

$$T_{Sm} = T_{Sol,M} + \frac{T_{Liq,M} - T_{Sol,M}}{h_{f,M}}(e_{Sm} - e_{Sol,M}),$$

$$e_{Sol,M} \le e_{Sm} < e_{Liq,M}, \qquad (1b)$$

where $a_{S1,M}$, $a_{S2,M}$ and $a_{S3,M}$ are the fitting constants, $u_{Sm} = \frac{e_{Sm}}{e_{Sol,M}}$ and $h_{f,M} = e_{Liq,M} - e_{Sol,M}$.

For the structure specific volume,

$$v_{Sm} = v_{Sol,M}[1 + b_{S1,M}(1-u_{Sm}) + b_{S2,M}(1-u_{Sm})^2 + b_{S3,M}(1-u_{Sm})^3],$$

$$e_{Sm} < e_{Sol,M}, \text{ and} \qquad (2a)$$

$$v_{Sm} = v_{Sol,M} + \frac{v_{Liq,M} - v_{Sol,M}}{h_{f,M}}(e_{Sm} - e_{Sol,M}),$$

$$e_{Sol,M} \le e_{Sm} < e_{Liq,M}, \qquad (2b)$$

where $b_{S1,M}$, $b_{S2,M}$ and $b_{S3,M}$ are the fitting constants. Equations (1b) and (2b) are used for extrapolation to the metastable state above the liquidus temperature.

For particles, such as fuel, steel and control, compression resulting from higher cell pressure, $p$, is assumed such that they can be treated similar to liquid, but otherwise obey structure functional relationships. The expressions for the particle temperature, $T_{Lm}$, and specific volume, $v_{Lm}$, are

$$T_{Lm} = T_{Lm}^{+} + \left(\frac{\partial T_{Lm}}{\partial p}\right)_M^{\circ} p, \text{ and} \qquad (3)$$

$$v_{Lm} = v^{+}_{Lm} + \left(\frac{\partial v_{Lm}}{\partial p}\right)^{\circ}_{M} p, \tag{4}$$

where a subscript Lm applies to particles this case. The terms with a "+" superscript in Eqs. (3) and (4) lack pressure dependence and apply to the sublimation curve of a solid state. The actual sublimation pressure is considered to be low enough to be ignored. The terms, $T^{+}_{Lm}$ and $v^{+}_{Lm}$, have the same energy-dependent curves as those for structure. The pressure derivatives, $\left(\frac{\partial T_{Lm}}{\partial p}\right)^{\circ}_{M}$ and $\left(\frac{\partial v_{Lm}}{\partial p}\right)^{\circ}_{M}$, are assumed to be constant independent of specific internal energy.

### *2.2. EOS functions for vapor properties*

#### *2.2.1. Vapor-pressure curve*

The saturated liquid vapor pressure, $p^{+}_{Lm}$, is defined as a function of liquid temperature, $T^{+}_{Lm}$:

$$p^{+}_{Lm} = \exp\left[b_{L1,M} + b_{L2,M}T^{+}_{Lm} + \frac{b_{L3,M}}{T^{+}_{Lm}} + b_{L4,M}\ln\left(\frac{T^{+}_{Lm}}{T_{Crt,M}}\right)\right]. \tag{5}$$

The constants, $b_{L1,M}$, $b_{L2,M}$, $b_{L3,M}$ and $b_{L4,M}$ in Eq. (5) can be fit or taken directly from the available data. The inverted saturated-vapor pressure curve is also used to calculate the saturation temperature, $T_{Sat,Gm}$, as a function of vapor pressure, $p_{Gm}$. The expression is

$$T_{Sat,Gm} = \frac{1}{a_{Sat1,M} + a_{Sat2,M}\ln p_{Gm} + a_{Sat3,M}(\ln p_{Gm})^2 + a_{Sat4,M}(\ln p_{Gm})^3}, \tag{6}$$

where $a_{Sat1,M}$, $a_{Sat2,M}$, $a_{Sat3,M}$ and $a_{Sat4,M}$ are the fitting constants. Equation (6) is fitted to the values calculated by Eq. (5) from the liquidus temperature to the critical temperature using the least-squares method.

#### *2.2.2. Modified Redlich-Kwong equations*

A modified Redlich-Kwong (MRK) equation (Fischer, 1992) is used for the vapor phase. The function form of the MRK equation is

$$p_{Gm} = \frac{R_M T_G}{v_{Gm} - a_{G1,M}} - \frac{a(T_G)}{v_{Gm}(v_{Gm} + a_{G3,M})}, \tag{7}$$

where

$$a(T_G) = a_{G2,M}\left(\frac{T_G}{T_{Crt,M}}\right)^{a_{G4,M}}, \qquad T_G < T_{Crt,M}, \text{ and} \tag{8a}$$

$$a(T_G) = a_{G2,M}\left[1 + a_{G4,M}\left(\frac{T_G}{T_{Cri,M}} - 1\right)\right], \qquad T_G \geq T_{Cri,M}. \tag{8b}$$

The EOS parameters, $a_{G1,M}$, $a_{G2,M}$, $a_{G3,M}$, in Eq. (7) are determined from the critical constants and the fact that the critical isotherm on a pressure-volume $p - v$ diagram has an inflection point at the critical point. Consequently, the first and second derivatives of the pressure with respect to specific volume are zero. The method to determine $a_{G4,M}$ is material dependent. It can be used to fit the slope of the vapor-pressure curve at the critical temperature, the Riedel factor (Riedel, 1954), or to obtain as best fit as possible to the vapor density. Equation (7) reduces to the van der Waals equation if $a_{G3,M} = 0$ and $a = const.$, and to the original Redlich-Kwong equation (Redlich and Kwong, 1949) if $a_{G1,M} = a_{G3,M}$ and $a_{G4,M} = -1/2$.

The MRK equation is practically simple similar to the well-known van der Waals equation, but it can be made reasonably accurate especially at high temperatures and reproduces the evaluated oxide fuel vapor data rather well (Fischer, 1992). It was found, however, that the MRK equation poorly reproduces the evaluated data of the internal energy and the heat capacity of sodium vapor. To solve this problem, it is newly proposed to extend the MRK equation to a reacting system (see Appendix A), which describes the dimerization of sodium vapor, and thereby satisfactory agreement is obtained (see Section 4.2). The proposed function form is

$$p_{Gm} = \frac{R_M T_G}{(1 + y_{B,Gm})(v_{Gm} - a_{G1,M})} - \frac{a(T_G)}{v_{Gm}(v_{Gm} + a_{G3,M})}. \tag{9}$$

In Eq. (9), $y_{B,Gm}$ is the dimer fraction expressed by

$$y_{B,Gm} = \frac{1 + 2x_{Gm} - \sqrt{1 + 8x_{Gm}}}{2(x_{Gm} - 1)}, \tag{10}$$

where

$$x_{Gm} = \frac{k_{2,Gm} R_M T_G}{v_{Gm} - a_{G1,M}}, \tag{11}$$

and $k_{2,Gm}$ is the equilibrium constant given by

$$k_{2,Gm} = \exp\left(d_{G1,M} + \frac{d_{G2,M}}{T_G}\right), \tag{12}$$

where $d_{G1,M}$ and $d_{G2,M}$ are the fitting constants.

The location where $\left(\frac{\partial p_{Gm}}{\partial v_{Gm}}\right)_{T_G}$ changes from negative to positive is called the limit of intrinsic stability or the spinodal limit (Carey, 1992). The spinodal curve is the locus of

spinodal limit points in the vapor dome and satisfies the following condition:

$$\left(\frac{\partial p_{Gm}}{\partial v_{Gm}}\right)_{T_G} = 0. \tag{13}$$

Here, the vapor specific volume on the spinodal curve, or spinodal volume, $v_{Spn,Gm}$, is defined as a function of vapor temperature. The proposed function form is

$$v_{Spn,Gm} = v_{Cri,M}\left[1 + f_{G1,M}(1-\eta_{G1,M})^{1/3} + f_{G2,M}(1-\eta_{G2,M}) + f_{G3,M}(1-\eta_{G3,M})^2 + f_{G4,M}(1-\eta_{G4,M})^5\right], \tag{14}$$

where $f_{G1,M}$, $f_{G2,M}$, $f_{G3,M}$ and $f_{G4,M}$ are the fitting constants and $\eta_{Gm} = \frac{T_G}{T_{Cri,M}}$.

The equation for the specific internal energy of vapor, $e_{Gm}$, is derived from the MRK equation for pressure to satisfy the following thermodynamic relation:

$$\left(\frac{\partial e_{Gm}}{\partial v_{Gm}}\right)_{T_G} = T_G\left(\frac{\partial p_{Gm}}{\partial T_G}\right)_{v_{Gm}} - p_{Gm}. \tag{15}$$

This gives

$$e_{Gm} = e^{+}_{Gm} + \frac{a(T_G) - T_G\frac{da}{dT_G}}{a_{G3,M}}\ln\left(\frac{1+\frac{a_{G3,M}}{v^{+}_{Gm}}}{1+\frac{a_{G3,M}}{v_{Gm}}}\right), \tag{16}$$

where $e^{+}_{Gm}$ and $v^{+}_{Gm}$ are reference values. The specific internal energy of vapor mixture is given by a mass-weighted average of the vapor material internal energies as

$$e_G = \frac{\sum_m \rho_{Gm} e_{Gm}}{\sum_m \rho_{Gm}}. \tag{17}$$

Using the specific volume and specific internal energy of infinitely dilute vapor as the reference values, the specific internal energy of vapor is given as a function of $T_G$ and $v_{Gm}$:

$$e_{Gm} = c_{vG,M}(T_G - T_{Liq,M}) + e^{D}_{LiqG,M} - \frac{a_{G2,M}(1-a_{G4,M})\psi}{a_{G3,M}}\ln\left(1+\frac{a_{G3,M}}{v_{Gm}}\right), \tag{18}$$

with

$$\psi = \left(\frac{T_G}{T_{Cri,M}}\right)^{a_{G4,M}}, \qquad T_G < T_{Cri,M}, \text{ and} \tag{19a}$$

$$\psi = 1, \qquad T_G \geq T_{Crt,M}. \tag{19b}$$

where $e^D_{LiqG,M}$ is the specific internal energy of infinitely dilute vapor at the liquidus temperature and $c_{vG,M}$ is the heat capacity at constant volume. For a reacting system, we apply the following equation derived from Eqs. (9) and (15):

$$e_{Gm} = c_{vG,M}(T_G - T_{Liq,M}) + e^D_{LiqG,M} + \frac{y_{B,Gm} R_M T_G}{1 + y_{B,Gm}}\left(1 - \frac{d_{G2,M}}{T_G}\right) - \frac{a_{G2,M}(1 - a_{G4,M})\psi}{a_{G3,M}} \ln\left(1 + \frac{a_{G3,M}}{\upsilon_{Gm}}\right). \tag{20}$$

In the equation for the specific internal energy of vapor, remaining unknown parameters are $c_{vG,M}$ and $e^D_{LiqG,M}$. The specific internal energy of saturated vapor, $e_{LiqG,M}$, at the liquidus temperature is determined from the Clapeyron equation:

$$h_{lg} = (\upsilon_{Gm,Sat} - \upsilon_{Lm,Sat}) T_{Sat} \left(\frac{dp}{dT}\right)_{Sat}, \tag{21}$$

where the heat of vaporization, $h_{lg}$, is given by

$$h_{lg} = h_{Gm,Sat} - h_{Lm,Sat} = (e_{Gm,Sat} + p_{Sat}\upsilon_{Gm,Sat}) - (e_{Lm,Sat} + p_{Sat}\upsilon_{Lm,Sat}). \tag{22}$$

Using the fact $\upsilon_{LiqG,M} >> \upsilon_{Liq,M}$, $e_{LiqG,M}$ is given by

$$e_{LiqG,M} \cong e_{Liq,M} + \upsilon_{LiqG,M}\left[T_{Liq,M}\left(\frac{dp}{dT}\right)_{Liq,M} - p_{Liq,M}\right]. \tag{23}$$

The value of $e^D_{LiqG,M}$ is then calculated from Eq. (18) or (20) using the evaluated $e_{LiqG,M}$. Generally, the value of $e^D_{LiqG,M}$ is almost equal to $e_{LiqG,M}$ at the liquidus temperature. The method to determine $c_{vG,M}$ is material dependent.

The vapor heat capacity at constant volume, $c_{vG,M}$, is calculated from Eq. (18):

$$c_{v,Gm} = \left(\frac{\partial e_{Gm}}{\partial T_G}\right)_{\upsilon_{Gm}} = c_{vG,M} - \frac{a_{G2,M}(1 - a_{G4,M})\psi^*}{a_{G3,M}} \ln\left(1 + \frac{a_{G3,M}}{\upsilon_{Gm}}\right), \tag{24}$$

where

$$\psi^* = \frac{a_{G4,M}}{T_{Crt,M}}\left(\frac{T_G}{T_{Crt,M}}\right)^{a_{G4,M}-1}, \qquad T_G < T_{Crt,M}, \text{ and} \tag{25a}$$

$$\psi^* = 0, \qquad T_G \geq T_{Crt,M}. \tag{25b}$$

For a reacting system, we obtain the following equation from Eq. (20):

$$c_{v,Gm} = c_{vG,M} - \frac{a_{G2,M}(1-a_{G4,M})\psi^*}{a_{G3,M}} \ln\left(1+\frac{a_{G3,M}}{\upsilon_{Gm}}\right)$$

$$+\frac{y_{B,Gm}R_M}{1+y_{B,Gm}}\left\{1+\frac{1-y_{B,Gm}}{1+3y_{B,Gm}}\left(1-\frac{d_{G2,M}}{T_G}\right)^2\right\}. \tag{26}$$

The vapor heat capacity at constant pressure, $c_{p,Gm}$, is expressed by the known thermodynamic relationships:

$$c_{p,Gm} = c_{v,Gm} - \frac{T_G\left(\frac{\partial p_{Gm}}{\partial T_G}\right)^2_{\upsilon_{Gm}}}{\left(\frac{\partial p_{Gm}}{\partial \upsilon_{Gm}}\right)_{T_G}}. \tag{27}$$

*2.2.3. Saturated vapor*

For the specific volume of saturated vapor, or vaporization volume, $\upsilon_{Vap,Gm}$, we select the following polynomial functional form originally used for water (Saul and Wanger, 1987):

$$\upsilon_{Vap,Gm} = \upsilon_{Crt,M}\exp[b_{G1,M}(1-\eta_{Sat,Gm})^{1/3} + b_{G2,M}(1-\eta_{Sat,Gm})^{2/3} + b_{G3,M}(1-\eta_{Sat,Gm})^{4/3}$$

$$+b_{G4,M}(1-\eta_{Sat,Gm})^3 + b_{G5,M}(1-\eta_{Sat,Gm})^{37/6} + b_{G6,M}(1-\eta_{Sat,Gm})^{71/6}],$$

$$T_{Sat,Gm} \leq T_{Crt,M}, \tag{28}$$

where $b_{G1,M}$, $b_{G2,M}$, $b_{G3,M}$, $b_{G4,M}$, $b_{G5,M}$ and $b_{G6,M}$ are the fitting constants and $\eta_{Sat,Gm} = \frac{T_{Sat,Gm}}{T_{Crt,M}}$.

This must be made thermodynamically consistent with the standard vapor-pressure curve and the MRK equations described in the previous section. Therefore, Eq. (5) and the MRK equation are first equated and numerically solved for the vapor specific volume.

The specific internal energy of saturated vapor, or the vaporization energy, $e_{Vap,Gm}$, is defined by the function:

$$e_{Vap,Gm} = e_{LiqG,M} + c_{G1,M}(T_{Sat,Gm} - T_{Liq,M}) + c_{G2,M}(T_{Sat,Gm} - T_{Liq,M})^2 + c_{G3,M}(T_{Sat,Gm} - T_{Liq,M})^3,$$

$$T_{Liq,M} < T_{Sat,Gm} \leq c_{G4,M}T_{Crt,M}, \text{ and} \tag{29a}$$

$$e_{Vap,Gm} = e_{Crt,M}[1 + c_{G5,M}(T_{Crt,M} - T_{Sat,Gm})^{1/2} + c_{G6,M}(T_{Crt,M} - T_{Sat,Gm})^2],$$

$$c_{G4,M}T_{Crt,M} < T_{Sat,Gm} \leq T_{Crt,M}, \tag{29b}$$

where $c_{G1,M}$, $c_{G2,M}$, $c_{G3,M}$, $c_{G4,M}$, $c_{G5,M}$ and $c_{G6,M}$ are the fitting constants. The value of $c_{G1,M}$ can be interpreted as a low-temperature heat capacity with $c_{G2,M}$ and $c_{G3,M}$ as correction terms. The vaporization energy is calculated from the specific internal energy of vapor with the vaporization volume obtained above.

### *2.3. EOS functions for liquid properties*

#### *2.3.1. Saturated liquid*

The function for the specific volume of saturated liquid, or condensate volume, $v_{Con,Gm}$, is given by

$$v_{Con,Gm} = v_{Liq,M}[1 + b_{Sat1,M}(T_{Sat,Gm} - T_{Liq,M}) + b_{Sat2,M}(T_{Sat,Gm} - T_{Liq,M})^2 + b_{Sat3,M}(T_{Sat,Gm} - T_{Liq,M})^3]^{-1},$$

$$T_{Liq,M} < T_{Sat,Gm} \leq b_{Sat4,M}T_{Crt,M}, \text{ and} \tag{30a}$$

$$v_{Con,Gm} = v_{Crt,M}[1 + b_{Sat5,M}(T_{Crt,M} - T_{Sat,Gm})^{1/2} + b_{Sat6,M}(T_{Crt,M} - T_{Sat,Gm})^2]^{-1},$$

$$b_{Sat4,M}T_{Crt,M} < T_{Liq,M} \leq T_{Crt,M}, \tag{30b}$$

where $b_{Sat1,M}$, $b_{Sat2,M}$, $b_{Sat3,M}$, $b_{Sat4,M}$, $b_{Sat5,M}$ and $b_{Sat6,M}$ are the fitting constants.

The expressions of the condensate energy, $e_{Con,Gm}$, defined as the specific internal energy of saturated liquid, are

$$e_{Con,Gm} = e_{Liq,M} + c_{Sat1,M}(T_{Sat,Gm} - T_{Liq,M}) + c_{Sat2,M}(T_{Sat,Gm} - T_{Liq,M})^2 + c_{Sat3,M}(T_{Sat,Gm} - T_{Liq,M})^3,$$

$$T_{Liq,M} < T_{Sat,Gm} \leq c_{Sat4,M}T_{Crt,M}, \text{ and} \tag{31a}$$

$$e_{Con,Gm} = e_{Crt,M}[1 - c_{Sat5,M}(T_{Crt,M} - T_{Sat,Gm})^{1/2} - c_{Sat6,M}(T_{Crt,M} - T_{Sat,Gm})^2],$$

$$c_{Sat4,M}T_{Crt,M} < T_{Sat,Gm} \leq T_{Crt,M}, \tag{31b}$$

where $c_{Sat1,M}$, $c_{Sat2,M}$, $c_{Sat3,M}$, $c_{Sat4,M}$, $c_{Sat5,M}$ and $c_{Sat6,M}$ are the fitting constants. The specific internal energy of saturated liquid is calculated from the Clapeyron equation, Eq. (21):

$$e_{Lm,Sat} = e_{Gm,Sat} - (v_{Gm,Sat} - v_{Lm,Sat})\left[T_{Sat}\left(\frac{dp}{dT}\right)_{Sat} - p_{Sat}\right], \tag{32}$$

where the saturation pressure and its derivative are calculated from Eq. (5). The specific volume and specific internal energy of saturated vapor are calculated as described in the previous section.

*2.3.2. Compressed liquid*

To assist in compressing each liquid to the cell pressure and to optimize the numerical algorithm for the pressure iteration, the independent EOS variables selected for the real liquid are pressure, $p$, and the component specific internal energy, $e_{Lm}$. We assume that temperature, $T_{Lm}$, and specific volume, $v_{Lm}$, can be defined by adding deviations from the saturation properties. The expressions for the liquid temperature and specific volume are

$$T_{Lm} = T^{+}_{Lm} + \left(\frac{\partial T_{Lm}}{\partial p}\right)_{e_{Lm}} (p - p^{+}_{Lm}), \text{ and} \tag{33}$$

$$v_{Lm} = v^{+}_{Lm} + \left(\frac{\partial v_{Lm}}{\partial p}\right)_{e_{Lm}} (p - p^{+}_{Lm}), \tag{34}$$

where $p^{+}_{Lm}$ is the saturation pressure corresponding to the liquid temperature, $T^{+}_{Lm}$, and is given by Eq. (5).

The saturated liquid temperature, $T^{+}_{Lm}$, and specific volume, $v^{+}_{Lm}$, are defined as a function of specific internal energy, $e_{Lm}$. The function for the saturated liquid temperature is expressed by

$$T^{+}_{Lm} = T_{Liq,M}[1 + a_{L1,M}(u_{Lm} - 1) + a_{L2,M}(u_{Lm} - 1)^2 + a_{L3,M}(u_{Lm} - 1)^3],$$

$$e_{Liq,M} < e_{Lm} \le a_{L4,M} e_{Liq,M}, \text{ and} \tag{35a}$$

$$T^{+}_{Lm} = T_{Crt,M}[1 - a_{L5,M}(1 - \xi_{Lm})^2 - a_{L6,M}(1 - \xi_{Lm})^3],$$

$$a_{L4,M} e_{Liq,M} < e_{Lm} \le e_{Crt,M}, \tag{35b}$$

where $a_{L1,M}$, $a_{L2,M}$, $a_{L3,M}$, $a_{L4,M}$, $a_{L5,M}$ and $a_{L6,M}$ are the fitting constants, and $u_{Lm} = \dfrac{e_{Lm}}{e_{Liq,M}}$ and $\xi_{Lm} = \dfrac{e_{Lm}}{e_{Crt,M}}$. For the liquid specific volume,

$$v^{+}_{Lm} = v_{Liq,M}[1 + d_{L1,M}(u_{Lm} - 1) + d_{L2,M}(u_{Lm} - 1)^2 + d_{L3,M}(u_{Lm} - 1)^3],$$

$$e_{Liq,M} < e_{Lm} \le d_{L4,M} e_{Liq,M}, \text{ and} \tag{36a}$$

$$v^{+}_{Lm} = v_{Crt,M}[1 + d_{L5,M}(1 - \xi_{Lm})^{1/2} + d_{L6,M}(1 - \xi_{Lm})^2],$$

$$d_{L4,M} e_{Liq,M} < e_{Lm} \le e_{Crt,M}, \tag{36b}$$

where $d_{L1,M}$, $d_{L2,M}$, $d_{L3,M}$, $d_{L4,M}$, $d_{L5,M}$ and $d_{L6,M}$ are the fitting constants.

*2.3.3. Pressure derivatives*

The pressure derivative of liquid temperature, $\left(\frac{\partial T_{Lm}}{\partial p}\right)_{e_{Lm}}$, in Eq. (33) is expressed by

$$\left(\frac{\partial T_{Lm}}{\partial p}\right)_{e_{Lm}} = \max\left\{\left(\frac{\partial T_{Lm}}{\partial p}\right)_{M}^{o}, f(\xi_{Lm})\right\}, \qquad e_{Lm} < e_{Crt,M}, \tag{37}$$

where

$$f(\xi_{Lm}) = \left(\frac{\partial T_{Lm}}{\partial p}\right)_{e_{Crt,M}} \exp[c_{L1,M}(1-\xi_{Lm}) + c_{L2,M}(1-\xi_{Lm})^{3/2} + c_{L3,M}(1-\xi_{Lm})^{2} + c_{L4,M}(1-\xi_{Lm})^{3}], \tag{38}$$

and $c_{L1,M}$, $c_{L2,M}$, $c_{L3,M}$ and $c_{L4,M}$ are the fitting constants. In Eq. (37), the constant lower limit, $\left(\frac{\partial T_{Lm}}{\partial p}\right)_{M}^{o}$, is used to be consistent with a pressure derivative for solid.

The pressure derivative of liquid specific volume, $\left(\frac{\partial v_{Lm}}{\partial p}\right)_{e_{Lm}}$, in Eq. (34) is expressed by

$$\left(\frac{\partial v_{Lm}}{\partial p}\right)_{e_{Lm}} = \min\left\{\left(\frac{\partial v_{Lm}}{\partial p}\right)_{M}^{o}, \max[g(\xi_{Lm}), f_{L6,M}]\right\}, \qquad e_{Lm} < e_{Crt,M}, \tag{39}$$

where

$$g(\xi_{Lm}) = f_{L1,M}\exp[f_{L2,M}(1-\xi_{Lm})^{-1/2} + f_{L3,M}(1-\xi_{Lm}) + f_{L4,M}(1-\xi_{Lm})^{3} + f_{L5,M}(1-\xi_{Lm})^{4}], \tag{40}$$

and $f_{L1,M}$, $f_{L2,M}$, $f_{L3,M}$, $f_{L4,M}$ and $f_{L5,M}$ are the fitting constants. In Eq. (39), the constant higher limit, $\left(\frac{\partial v_{Lm}}{\partial p}\right)_{M}^{o}$, is also used to be consistent with the solid value.

The partial derivatives, $\left(\frac{\partial T_{Lm}}{\partial p}\right)_{e_{Lm}}$ and $\left(\frac{\partial v_{Lm}}{\partial p}\right)_{e_{Lm}}$, at constant internal energy in Eqs. (33) and (39) are related to commonly used derivatives as follows:

$$\left(\frac{\partial T_{Lm}}{\partial p}\right)_{e_{Lm}} = \left\{\left(\frac{\partial p}{\partial T_{Lm}}\right)_{v_{Lm}} - \frac{c_{v,Lm}\left(\frac{\partial p}{\partial v_{Lm}}\right)_{T_{Lm}}}{T_{Lm}\left(\frac{\partial p}{\partial T_{Lm}}\right)_{v_{Lm}} - p}\right\}^{-1}, \text{ and} \tag{41}$$

$$\left(\frac{\partial v_{\mathrm{Lm}}}{\partial p}\right)_{e_{\mathrm{Lm}}} = \left\{\left(\frac{\partial p}{\partial v_{\mathrm{Lm}}}\right)_{T_{\mathrm{Lm}}} - \left(\frac{\partial p}{\partial T_{\mathrm{Lm}}}\right)_{v_{\mathrm{Lm}}} \frac{T_{\mathrm{Lm}}\left(\frac{\partial p}{\partial T_{\mathrm{Lm}}}\right)_{v_{\mathrm{Lm}}} - p}{c_{\mathrm{v,Lm}}}\right\}^{-1}, \tag{42}$$

where

$$c_{\mathrm{v,Lm}} = \left(\frac{\partial e_{\mathrm{Lm}}}{\partial T_{\mathrm{Lm}}}\right)_{v_{\mathrm{Lm}}}, \tag{43}$$

is the heat capacity at constant volume of a liquid. With the following thermodynamic relationships:

$$T_{\mathrm{Lm}}\left(\frac{\partial p}{\partial T_{\mathrm{Lm}}}\right)_{v_{\mathrm{Lm}}} - p = \frac{\left(\frac{de_{\mathrm{Lm}}}{dT}\right)_{\mathrm{Sat}} - c_{\mathrm{v,Lm}}}{\left(\frac{dv_{\mathrm{Lm}}}{dT}\right)_{\mathrm{Sat}}}, \text{ and} \tag{44}$$

$$\left(\frac{\partial p}{\partial v_{\mathrm{Lm}}}\right)_{T_{\mathrm{Lm}}} = \frac{\left(\frac{dp}{dT}\right)_{\mathrm{Sat}} - \left(\frac{dp}{dT_{\mathrm{Lm}}}\right)_{v_{\mathrm{Lm}}}}{\left(\frac{dv_{\mathrm{Lm}}}{dT}\right)_{\mathrm{Sat}}}, \tag{45}$$

which hold on the saturation line, Eqs. (41) and (42) can be expressed by $c_{\mathrm{v,Lm}}$ and the derivatives along the saturation line. A derivative, $\left(\frac{de_{\mathrm{Lm}}}{dT}\right)_{\mathrm{Sat}}$, on the right hand side of Eq. (44) is derived from the Clapeyron equation as follows:

$$\left(\frac{de_{\mathrm{Lm}}}{dT}\right)_{\mathrm{Sat}} = \left(\frac{de_{\mathrm{Gm}}}{dT}\right)_{\mathrm{Sat}} - [T_{\mathrm{Sat}}\left(\frac{dp}{dT}\right)_{\mathrm{Sat}} - p_{\mathrm{Sat}}][\left(\frac{dv_{\mathrm{Gm}}}{dT}\right)_{\mathrm{Sat}} - \left(\frac{dv_{\mathrm{Lm}}}{dT}\right)_{\mathrm{Sat}}]$$

$$-T_{\mathrm{Sat}}(v_{\mathrm{Gm,Sat}} - v_{\mathrm{Lm,Sat}})\left(\frac{d^2p}{dT^2}\right)_{\mathrm{Sat}}, \tag{46}$$

where a derivative, $\left(\frac{de_{\mathrm{Gm}}}{dT}\right)_{\mathrm{Sat}}$, can be obtained from the following thermodynamic relations:

$$\left(\frac{de_{\mathrm{Gm}}}{dT}\right)_{\mathrm{Sat}} = \left(\frac{\partial e_{\mathrm{Gm}}}{\partial T_{\mathrm{G}}}\right)_{v_{\mathrm{Gm}}} + \left(\frac{\partial e_{\mathrm{Gm}}}{\partial v_{\mathrm{Gm}}}\right)_{T_{\mathrm{G}}}\left(\frac{dv_{\mathrm{Gm}}}{dT}\right)_{\mathrm{Sat}}, \text{ and} \tag{47}$$

$$\left(\frac{dv_{Gm}}{dT}\right)_{Sat} = \frac{\left(\frac{dp}{dT}\right)_{Sat} - \left(\frac{\partial p_{Gm}}{\partial T_G}\right)_{v_{Gm}}}{\left(\frac{\partial p_{Gm}}{\partial v_{Gm}}\right)_{T_G}}. \tag{48}$$

In Eqs. (47) and (48), partial derivatives of vapor pressure and specific internal energy can be calculated from the MRK EOS.

A remaining unknown variable is $c_{v,Lm}$ for the calculation of Eqs. (41) and (42). From a well-known thermodynamic relationship, we can write

$$c_{v,Lm} = \frac{\beta_{S,Lm}}{\beta_{T,Lm}} c_{p,Lm}, \tag{49}$$

where

$$c_{p,Lm} = \left(\frac{\partial h_{Lm}}{\partial T_{Lm}}\right)_p, \tag{50}$$

is the heat capacity at constant pressure of a liquid,

$$\beta_{S,Lm} = -\frac{1}{v_{Lm}}\left(\frac{\partial v_{Lm}}{\partial p}\right)_{S_{Lm}}, \tag{51}$$

is the adiabatic compressibility of a liquid, and

$$\beta_{T,Lm} = -\frac{1}{v_{Lm}}\left(\frac{\partial v_{Lm}}{\partial p}\right)_{T_{Lm}}, \tag{52}$$

is the isothermal compressibility of a liquid. Chawla et al. (1981) have used the following equation by Rowlinson and Swinton (1982) for the calculation of the isothermal compressibility:

$$\beta_{T,Lm} = \frac{\beta_{S,Lm} c_{Sat,Lm} + v_{Lm} T_{Lm} \alpha_{Sat,Lm} [\alpha_{Sat,Lm} + \beta_{S,Lm} \left(\frac{dp}{dT}\right)_{Sat}]}{c_{Sat,Lm} - v_{Lm} T_{Lm} \left(\frac{dp}{dT}\right)_{Sat} [\alpha_{Sat,Lm} + \beta_{S,Lm} \left(\frac{dp}{dT}\right)_{Sat}]}, \tag{53}$$

where $c_{Sat,Lm}$ is the heat capacity along the saturation curve and is defined as

$$c_{Sat,Lm} = \left(\frac{dh_{Lm}}{dT}\right)_{Sat} - v_{Lm}\left(\frac{dp}{dT}\right)_{Sat}, \tag{54}$$

and $\alpha_{Sat,Lm}$ is the volumetric thermal expansion coefficient along the saturation curve and is defined as

$$\alpha_{\mathrm{Sat,Lm}} = \frac{1}{v_{\mathrm{Lm}}}\left(\frac{dv_{\mathrm{Lm}}}{dT}\right)_{\mathrm{Sat}}. \tag{55}$$

Equation (54) is rewritten by the relation, $h = e + pv$, as follows:

$$c_{\mathrm{Sat,Lm}} = \left(\frac{de_{\mathrm{Lm}}}{dT}\right)_{\mathrm{Sat}} + p\left(\frac{dv_{\mathrm{Lm}}}{dT}\right)_{\mathrm{Sat}}. \tag{56}$$

The value of $\beta_{\mathrm{S,Lm}}$ is calculated from the speed of sound using the relation

$$\beta_{\mathrm{S,Lm}} = \frac{v_{\mathrm{Lm}}}{v_{\mathrm{S,Lm}}^{\,2}}, \tag{57}$$

where $v_{\mathrm{S,Lm}}$ is the speed of sound in the liquid state. The liquid heat capacity at constant pressure, $c_{\mathrm{p,Lm}}$, is expressed by a well-known thermodynamic relationship:

$$c_{\mathrm{p,Lm}} = c_{\mathrm{Sat,Lm}} + v_{\mathrm{Lm}} T_{\mathrm{Lm}} \alpha_{\mathrm{p,Lm}} \left(\frac{dp}{dT}\right)_{\mathrm{Sat}}, \tag{58}$$

where

$$\alpha_{\mathrm{p,Lm}} = \frac{1}{v_{\mathrm{Lm}}}\left(\frac{\partial v_{\mathrm{Lm}}}{\partial T_{\mathrm{Lm}}}\right)_{p}, \tag{59}$$

is the volumetric thermal expansion coefficient of a liquid. The value of $\alpha_{\mathrm{p,Lm}}$ is calculated from the following equation (Chawla et al., 1981):

$$\alpha_{\mathrm{p,Lm}} = \alpha_{\mathrm{Sat,Lm}} + \beta_{\mathrm{T,Lm}}\left(\frac{dp}{dT}\right)_{\mathrm{Sat}}. \tag{60}$$

In Eq. (38), a value of $\left(\frac{\partial T_{\mathrm{Lm}}}{\partial p}\right)_{e_{\mathrm{Cri,M}}}$ for the critical point is obtained from the MRK equations as follows:

$$\left(\frac{\partial T_{\mathrm{Lm}}}{\partial p}\right)_{e_{\mathrm{Cri,M}}} = \left(\frac{\partial p_{\mathrm{Gm}}}{\partial T_{\mathrm{G}}}\right)^{-1}_{v_{\mathrm{Cri,M}}}. \tag{61}$$

In Eq. (39), the lower limiting value, $f_{\mathrm{L6,M}}$, is numerically required and is obtained from the MRK EOS using the vapor heat capacity, $\left(\frac{\partial e_{\mathrm{Gm}}}{\partial T_{\mathrm{G}}}\right)_{v_{\mathrm{Cri,M}}}$, calculated at the critical point instead of $c_{\mathrm{v,Lm}}$:

$$f_{L6,M} = -\left\{ \left( \frac{\partial p_{Gm}}{\partial T_G} \right)_{v_{Cri,M}} \frac{T_{Cri,M} \left( \frac{\partial p_{Gm}}{\partial T_G} \right)_{v_{Cri,M}} - p_{Cri,M}}{\left( \frac{\partial e_{Gm}}{\partial T_G} \right)_{v_{Cri,M}}} \right\}^{-1} . \quad (62)$$

As mentioned above, the pressure derivatives for solid, $\left( \frac{\partial T_{Lm}}{\partial p} \right)_M^o$ and $\left( \frac{\partial v_{Lm}}{\partial p} \right)_M^o$, are assumed to be constant independent of specific internal energy. These can be approximated by

$$\left( \frac{\partial T_{Lm}}{\partial p} \right)_M^o = \frac{\beta_{T,Sm}}{\alpha_{p,Sm}}, \text{ and} \quad (63)$$

$$\left( \frac{\partial v_{Lm}}{\partial p} \right)_M^o = -v_{Sm} \beta_{S,Sm}, \quad (64)$$

or the values at the melting point calculated from the fitted equations (38) and (40), where

$$\alpha_{p,Sm} = \frac{1}{v_{Sm}} \left( \frac{\partial v_{Sm}}{\partial T_{Sm}} \right)_p, \quad (65)$$

is the volumetric thermal expansion coefficient of a solid,

$$\beta_{T,Sm} = -\frac{1}{v_{Sm}} \left( \frac{\partial v_{Sm}}{\partial p} \right)_{T_{Sm}}, \quad (66)$$

is the isothermal compressibility of a solid, and

$$\beta_{S,Sm} = -\frac{1}{v_{Sm}} \left( \frac{\partial v_{Sm}}{\partial p} \right)_{S_{Sm}}, \quad (67)$$

is the adiabatic compressibility of a solid.

## Chapter 3. EOS treatment in pressure iteration

The EOS modeling is also a very important concern in designing the algorithm for pressure iteration to obtain consistency between end-of-time-step pressures and other sensitive variables. The pressure iteration in SIMMER–II (Bohl and Luck, 1990) attempted to obtain consistent velocities and pressures that reduced the error to near zero in the overall liquid continuity equation (for single-phase cells) or the overall vapor continuity equation (for two-phase cells) assuming that derivatives in densities with respect to pressure were constant. This approach resulted in inaccuracies in some situations such as generating spurious pressure spikes at two-phase/single-phase boundaries. In AFDM (Bohl et al., 1990), an inner EOS iteration was implemented to obtain mechanical equilibrium to compress each liquid to a state that is consistent with an identical pressure, and thereby to define the vapor volume fraction. In this algorithm, an EOS pressure, $p_{EOS}$, is determined by the thermodynamic state of the cell components alone, and is expressed by

$$p_{EOS} = f(\overline{\rho}_{Gm}, T_G, \overline{\rho}_{Lm}, T_{Lm}, \alpha_S), \quad \text{for a two-phase cell, and} \tag{68}$$

$$p_{EOS} = f(\overline{\rho}_{Lm}, T_{Lm}, \alpha_S), \quad \text{for a single-phase cell,} \tag{69}$$

where $\alpha_S$ is the overall structure volume fraction, and $\overline{\rho}_{Lm}$ is the macroscopic density of a liquid component. This treatment, together with time-consuming table search and interpolation, significantly deteriorated the computing efficiency of AFDM. In SIMMER–III a new method is introduced to eliminate the inner EOS iteration by relating the cell pressure, $p_{CELL}$, to the amount of liquid compression. That is, two-phase pressure, $p_G$, and single-phase pressure, $p_{1\phi}$, are given by

$$p_G = f(\overline{\rho}_{Gm}, T_G, \overline{\rho}_{Lm}, e_{Lm}, \alpha_S, p_{CELL}), \text{ and} \tag{70}$$

$$p_{1\phi} = f(\overline{\rho}_{Lm}, e_{Lm}, \alpha_S, p_{CELL}). \tag{71}$$

With this method, the mechanical equilibrium among liquid components with the cell pressure is automatically guaranteed when the pressure iteration is converged. The objective of the SIMMER–III pressure iteration is to adjust the macroscopic densities, the cell-edge velocities, the vapor temperature, and the cell pressure such that the following six sensitive quantities are reduced to negligible values. These include the difference between the cell pressure and the EOS pressure, the errors in the mass conservation equations, and the error in the vapor temperature. This selection was based on the experience and lessons learned in AFDM.

The EOS pressure must account for both the single-phase and two-phase situations, and is modeled as follows. First, the liquid-field volume fraction, $\alpha_L$, and vapor-field volume fraction, $\alpha_G$, are calculated using $v_{Lm}$ computed by Eqs. (4) and (34):

$$\alpha_L = \sum_m \alpha_{Lm}, \tag{72}$$

where

$$\alpha_{Lm} = \overline{\rho}_{Lm} \upsilon_{Lm}, \text{ and} \tag{73}$$

$$\alpha_G = (1 - \alpha_S) - \alpha_L, \tag{74}$$

where $\alpha_L$ is fixed during a pressure iteration. To avoid a numerical problem, two-phase to single-phase transition is assumed to occur at a small, non-zero vapor volume fraction, $\alpha_0$. The formalism adopted assumes that vapor exists in every cell with an effective vapor-volume fraction, $\alpha_{ge}$. This is defined such that conversion of structure into a liquid field component would not change the pressure. Thus an effective vapor-volume fraction and vapor microscopic densities are calculated as

$$\alpha_{ge} = \max[\alpha_0(1 - \alpha_S), \alpha_G + \alpha_0 \alpha_L], \text{ and} \tag{75}$$

$$\rho_{Gm} = \frac{\overline{\rho}_{Gm}}{\alpha_{ge}}. \tag{76}$$

The vapor-component partial pressures, $p_{Gm}$, are then determined from the MRK equation, with the total vapor-field pressure being assumed to obey Dalton's law:

$$p_G = \sum_m p_{Gm}. \tag{77}$$

If a cell is overfilled with liquid such that $\alpha_G < 0$, $p_{CELL}$ must be increased to compress the liquid volume. This is accomplished by expanding $\alpha_G$ with $p_{CELL}$ as

$$\alpha_G + \frac{\partial \alpha_G}{\partial p_{CELL}}(p_{1\phi} - p_{CELL}) = 0. \tag{78}$$

Equation (78) is solved to obtain a single-phase pressure by

$$p_{1\phi} = p_{CELL} - \alpha_G \left( \frac{\partial \alpha_G}{\partial p_{CELL}} \right)^{-1}. \tag{79}$$

Then, for all cells in any stage of iteration

$$p_{EOS} = \max(p_G, p_{1\phi}). \tag{80}$$

The values of vapor volume fraction corresponding to $p_{EOS}$ is

$$\alpha_{G,EOS} = \alpha_G, \qquad \text{if } p_{EOS} = p_G, \text{ and} \tag{81}$$

$$\alpha_{G,EOS} = -10^{-20}, \qquad \text{if } p_{EOS} = p_{1\phi}. \tag{82}$$

A cell is two phase if $\alpha_{G,EOS} > 0$, or single phase if $\alpha_{G,EOS} = -10^{-20}$. It is possible to have $\alpha_G < 0$ and $p_G > p_{l\phi}$, or $\alpha_G > 0$ and $p_G < p_{l\phi}$; however, this condition should be corrected by the reduction of the difference between the $p_{CELL}$ and $p_{EOS}$ to zero resulting in contraction/expansion of the liquids. Once convergence is obtained, a two-phase cell should have $\alpha_G \geq 0$. A single-phase cell should have $\alpha_G < 0$, which can be reasonably set to $-10^{-20}$. Once $p_{EOS}$ is defined and $\alpha_{G,EOS}$ is set to define the cell two-phase or single-phase condition, Eqs. (75) and (76) are used to obtain new vapor microscopic densities (specific volumes).

## Chapter 4. Properties of reactor materials

In this chapter, thermodynamic properties of the basic reactor-core materials such as oxide fuel, stainless steel, and sodium are newly evaluated using compilation of the most up-to-date and reliable sources available at present. As described previously, the vapor properties can be determined by the $p-v-T$ relationships based on the MRK equation. The liquid-side EOS data along the saturation curve also can be evaluated consistently with the thermodynamic relations using the MRK equation on the vapor side and the Clapeyron equation. The previously published and compiled thermodynamic data of oxide fuel, stainless steel, and sodium, which are used as the basis of EOS data developed in this study, are summarized as follows.

An important task has been completed at Forschungszentrum Karlsruhe (FZK) to provide the new EOS data of oxide fuel (Fischer, 1987, 1989). A complete new evaluation of the EOS of uranium oxide was carried out between the melting point and the critical point. In the FZK study the Significant Structure Theory (SST) was applied, extended to the case of non-stoichiometric urania and good agreement of the evaluated EOS with the recent experimental data (R. Limon et al., 1981; Ohse et al., 1985; Bober and Singer, 1987; Breitung and Reil, 1989, 1990) was obtained. This is additional evidence for the reliability and consistency of the recent data. Analytic data fits for the important state variables were also proposed for convenient use in the fast reactor accident analysis codes (Fischer, 1992). In this study, the EOS data of uranium dioxide and mixed oxide on liquid and vapor sides are reproduced based on the new evaluation. On thermodynamic properties of solid fuel such as enthalpy and density, we adopt the previously compiled data by the Argonne National Laboratory (ANL) group (Fink and Petri, 1997) for uranium dioxide, and by Harding et al. (1989) and the ANL group (private communication with Fink, J.K.) for mixed oxide.

For stainless steel, due to insufficient experimental data, some of the properties have been either obtained by extrapolating actual experimental data from a low temperature range or estimated with thermodynamic theory and empirical relations (Kim, 1975; Chawla et al., 1981). The only available data for vapor-pressure values were the curves of type 304 and type 316 stainless steels theoretically evaluated by Kim (1975) on the basis of Raoult's low, until Bober and Singer (1985) have experimentally determined the vapor-pressure curve of type 1.4970 stainless steel in the temperature range between 2800-3900 K. Kim also obtained the properties in a solid state by extrapolating available experimental data to the melting point, while he used empirical rules to estimate the properties in a liquid state. In the latter calculations, corresponding properties of individual steel components needed to be extrapolated from temperatures around the melting point up to several thousand Kelvin. It seems, however, that relatively few studies have been made thus far on the properties of stainless steel from the viewpoint of reactor safety analysis. Accordingly, little reliable sources are available for use

in the LMFR safety analysis due to lack of the experimental data of stainless steel as well as steel components in a high temperature region. On the other hand, the new thermodynamic data for American Iron and Steel Institute (AISI) type 316 stainless steel are proposed in this study, based on a new compilation of properties of transition metals (Thurnay. K., Unpublished report, Kernforschungszentrum Karlsruhe, July 1991). Major thermodynamic properties of stainless steel such as the vapor-pressure curve, the enthalpy in the solid state, the density in the solid and liquid states are evaluated, assuming the ideal mixture and using the appropriate empirical relations. The extrapolation of the evaluated data to a critical temperature is carried out so as to obtain thermodynamically consistent liquid EOS data using the MRK equation on a vapor side.

For sodium, thermodynamic properties assessed by the ANL group (Fink and Leibowitz, 1995; 1996), are adopted as a data basis: the vapor-pressure curve, the critical parameters, the liquid density, and the adiabatic compressibility of the liquid. The ANL group has been performed a consistent assessment of sodium properties to include new information since their previous review (Fink and Leibowitz, 1982). They obtained consistent equations for the thermodynamic properties of saturated sodium, which have physically proper behavior from the melting point to the critical point. For the vapor-side EOS, the MRK equation extended to a reacting system, as described in Section 2.2, is used to complete the data necessary for the EOS functions.

### *4.1. Solid properties*

#### *A. Fuel*

The melting point of stoichiometric, unirradiated $UO_2$, has been taken as 3120±30 K, as recommended in an IAEA assessment by Rand et al. (1978). We apply this value to the solidus and liquidus temperatures of $UO_2$:

$$T_{\mathrm{Sol,M}} = T_{\mathrm{Liq,M}} = 3120\ \mathrm{K}.$$

The ANL group recommended the following equations to represent the enthalpy of solid $UO_2$ relative to the enthalpy at 298.15 K:

$$h_s = C_1\theta\left[\left\{\exp\left(\frac{\theta}{T}\right)-1\right\}^{-1} - \left\{\exp\left(\frac{\theta}{298.15}\right)-1\right\}^{-1}\right]$$

$$+C_2(T^2-298.15^2)+C_3k\left[T\exp\left(-\frac{E_a}{k_BT}\right)-298.15\exp\left(-\frac{E_a}{298.15k_B}\right)\right],$$

$$273\ \mathrm{K} \le T \le 2670\ \mathrm{K}, \text{ and} \qquad (83a)$$

$$h_s = 167.04T - 218342\ , \qquad 273\ \mathrm{K} \le T \le 3120\ \mathrm{K}, \qquad (83b)$$

where $\theta$ = 516.12 K, $C_1$ = 78.215 J mol$^{-1}$ K, $C_2 = 3.8609 \times 10^{-3}$ J mol$^{-1}$ K$^{-2}$, $C_3 = 3.4250 \times 10^{8}$ J mol$^{-1}$ eV$^{-1}$, $E_a$ = 1.9105 eV, $k_B = 8.6144 \times 10^{-5}$ eV K$^{-1}$ is the Boltzmann constant, $T$ is in K, and $h_s$ is in J mol$^{-1}$. Equation (83b) gives the specific internal energy at the solidus temperature:

$e_{Sol,M} = 1.12157 \times 10^{6}$ J kg$^{-1}$.

From the heat of fusion value, $h_f$ = 74.83 kJ mol$^{-1}$, for $UO_2$ by the ANL group, we obtain the specific internal energy at the liquidus temperature:

$e_{Liq,M} = 1.39871 \times 10^{6}$ J kg$^{-1}$.

For the density of solid $UO_2$, the ANL group recommended to use the following equation as a function of temperature:

$$\rho_s(T) = \rho_s(273)\left(\frac{L(273)}{L(T)}\right)^3, \tag{84}$$

where the density at 273 K, $\rho_s(273)$, is equal to 10963 kg m$^{-3}$; $L(273)$ and $L(T)$ are the lengths at 273 K and at temperature T (K), respectively. They recommended the following fit by Martin (1988) for the linear thermal expansion of solid $UO_2$:

$$L(T) = L(273)\left(9.9734 \times 10^{-1} + 9.802 \times 10^{-6} T - 2.705 \times 10^{-10} T^2 + 4.391 \times 10^{-13} T^3\right),$$

$$273 \text{ K} \le T \le 923 \text{ K, and} \tag{85a}$$

$$L(T) = L(273)\left(9.9672 \times 10^{-1} + 1.179 \times 10^{-5} T - 2.429 \times 10^{-9} T^2 + 1.219 \times 10^{-12} T^3\right),$$

$$923 \text{ K} \le T \le 3120 \text{ K}. \tag{85b}$$

Equation (84) yields the specific volume at the solidus temperature:

$v_{Sol,M} = 1.04656 \times 10^{-4}$ m$^3$ kg$^{-1}$.

From the Drotning's data (Drotning, 1982) for the liquid density of $UO_2$ at the melting point, $\rho_m = 8860 \pm 120$ kg m$^{-3}$, we obtain the specific volume at the liquidus temperature:

$v_{Liq,M} = 1.12867 \times 10^{-4}$ m$^3$ kg$^{-1}$.

Adamson et al. (1985) gave the solidus and liquidus curves of stoichiometric $UO_2$–$PuO_2$ solutions represented by the following polynomial expressions, incorporating the IAEA-recommended melting point of $UO_2$ and adopting the melting point of $PuO_2$ as 2701 ± 35 K:

$$T_{Sol} = 3120.0 - 655.3y + 336.4y^2 - 99.9y^3, \text{ and} \tag{86a}$$

$$T_{\mathrm{Liq}} = 3120.0 - 388.1y - 30.4y^2, \qquad (86b)$$

where $y$ is the mole fraction of $PuO_2$. For the mixed oxide with 20 % mole fraction of $PuO_2$, Eqs. (86) give

$$T_{\mathrm{Sol.M}} = 3002\ \mathrm{K} \quad \text{and} \quad T_{\mathrm{Liq.M}} = 3041\ \mathrm{K}.$$

Harding et al. (1989) presented a mole-averaging scheme to obtain the enthalpy of solid mixed oxide by a suitable interpolation between $UO_2$ and $PuO_2$ data:

$$h_s(U_{1-y}Pu_yO_2) = y\,h_s(PuO_2) + (1-y)h_s(UO_2). \qquad (87)$$

They obtained the following expressions for the enthalpy relative to the solid at 298 K:

($UO_2$)

$$h_s = -22528 + 201296\tau + 138884\tau^2 + 5498.6\tau^3 - 329758\tau^4 + 322837\tau^5 + 186.3\tau^{-1},$$

$$\tau \le 0.856, \text{ and} \qquad (88a)$$

$$h_s = 521159\tau - 220041, \qquad \tau > 0.856. \qquad (88b)$$

($PuO_2$)

$$h_s = -32481 + 228656\tau + 43346\tau^2 - 11270\tau^3 + 987.72\tau^4 + 1970.7\tau^5 + 744.21\tau^{-1},$$

$$\tau \le 0.856, \text{ and} \qquad (89a)$$

$$h_s = 352544\tau - 109876, \qquad \tau > 0.856. \qquad (89b)$$

In the above equations, $\tau$ is the reduced temperature, $T/T_m$, where $T_m$ is the melting temperature of the solid, and $h_s$ is in J $mol^{-1}$. Harding et al. assumed that the melting points of the mixed oxide fuels may be obtained by linear interpolation. Note that Eqs. (88) for the solid $UO_2$ data are consistent with the results by the ANL group, Eqs. (83). From Eq. (87) we obtain the specific internal energy at the solidus temperature for the mixed oxide with $y$ = 0.2:

$$e_{\mathrm{Sol.M}} = 1.05162 \times 10^6\ \mathrm{J\ kg^{-1}}.$$

Harding et al. also gave the following expression to obtain the heat of fusion value in J $mol^{-1}$ for the mixed oxide as a function of mole fraction of $PuO_2$:

$$h_f = 76537.9 + 3581.5y\ . \qquad (90)$$

Equation (90), however, is inconsistent with the value for $UO_2$ obtained by the ANL group. They calculated the heat of fusion value for $UO_2$–$PuO_2$ compositions from the relationship

$$h_f(\mathrm{MOX}) = \frac{h_f(\mathrm{UO_2})}{T_m(\mathrm{UO_2})} T_m(\mathrm{MOX}), \qquad (91)$$

where $T_m$ is the melting temperature, which is taken as the solidus temperature for the mixed oxide (MOX) compositions. The above equation yields $h_f$ = 72.00 kJ mol$^{-1}$ for the mixed oxide with 20 % mole fraction of $PuO_2$ and hence the specific internal energy at the liquidus temperature is given by

$e_{\mathrm{Liq.M}} = 1.31829 \times 10^6$ J kg$^{-1}$.

The density for $(U_{1-y}, Pu_y)O_{2-x}$ compositions is not only dependent on Pu content, but also oxygen-to-metal ratio (O/M). For the density of solid $(U_{0.8}, Pu_{0.2})O_{1.98}$, the ANL group recommended the following cubic equation:

$$\rho_s = 11006 \times (1.0055 - 1.2498 \times 10^{-5} T - 1.9530 \times 10^{-8} T^2 + 4.2334 \times 10^{-12} T^3). \qquad (92)$$

where is in $T$ is in K, and $\rho_s$ is in J mol$^{-1}$. The above equation yields the specific volume at the solidus temperature:

$v_{\mathrm{Sol.M}} = 1.00230 \times 10^{-4}$ m$^3$ kg$^{-1}$.

From $\rho_s = 9.19 \times 10^{-3}$ kg m$^{-3}$ for $(U_{0.8}, Pu_{0.2})O_{1.98}$ at the liquidus temperature recommended by the ANL group, we obtain the specific volume at the liquidus temperature:

$v_{\mathrm{Liq.M}} = 1.08814 \times 10^{-4}$ m$^3$ kg$^{-1}$.

*B. Stainless steel*

Type 316 stainless steel is an alloy of Fe, Cr, Ni, Mo and a small amount of C. On the average it contains 69% Fe, 17% Cr, 12% Ni and 2% Mo by weight. According to this composition, type 316 stainless steel has an average molecular weight of

$W_M = 55.9354 \times 10^{-3}$ kg mol$^{-1}$.

The following liquidus and solidus temperatures are recommended, which were experimentally obtained for a stainless steel with a similar composition to type 316 stainless steel by Kurz and Lux (1969):

$T_{\mathrm{Sol.M}} = 1713$ K and $T_{\mathrm{Liq.M}} = 1753$ K.

Based on the enthalpy in the solid region and the heat of fusion estimated by the additivity rule assuming the ideal mixture (Belton and Fruehan, 1970), the following specific internal energies are recommended for type 316 stainless steel at its liquidus and solidus points:

$e_{\mathrm{Sol.M}} = 9.12379 \times 10^5$ J kg$^{-1}$ and $e_{\mathrm{Liq.M}} = 1.25158 \times 10^6$ J kg$^{-1}$.

where the specific internal energy is based on the enthalpy relative to the solid at 298.15 K. The theoretical densities of type 316 stainless steel in the solid and liquid states were evaluated on the basis of a formula which gives the specific volume of an ideal mixture as a mass-weighted average of the specific volumes of constituent elements (Hull, 1969). The resulting specific volumes at the liquidus and solidus points are

$$\upsilon_{Sol,M} = 1.36168 \times 10^{-4}\ m^3\ kg^{-1} \quad \text{and} \quad \upsilon_{Liq,M} = 1.41420 \times 10^{-4}\ m^3\ kg^{-1}.$$

*4.2. Vapor Properties*

*4.2.1. Vapor-pressure curve and critical data*

*A. Fuel*

Analytical fits were proposed for the vapor-pressure curve of stoichiometric $UO_2$ (Fischer, 1989). The total pressure is composed of the pressure of the urania-bearing species and the partial pressure of oxygen. The total pressure (including oxygen) is expressed by

$$\log p_{tot} = 47.287 - \frac{36269}{T} + 0.3615 \times 10^{-3} T - 4.8665 \ln(T), \tag{93}$$

and for the pressure of the urania-bearing species (saturation pressure)

$$\log p_{Sat} = 39.187 - \frac{34715}{T} + 0.1921 \times 10^{-3} T - 3.8571 \ln(T), \tag{94}$$

where $p$ is in MPa and $T$ is in K. While the total pressure is the true physical pressure, only the saturation pressure is consistent with thermodynamic relationships, e.g. the Clapeyron equation. Up to about 7000 K the contribution of oxygen to the total pressure is not so large and lies within the uncertainty band over the range where experimental data exist. Beside, it was recommended to use the vapor-pressure curve of $UO_2$ in accident analysis for mixed-oxide fueled fast reactors because no noteworthy differences were detected between the vapor pressure of $UO_2$ and mixed oxide in the experiments by Breitung and Reil (1989). We use, therefore, the saturation pressure curve, Eq. (94), for both $UO_2$ and mixed oxide. The following critical point data of stoichiometric $UO_2$ were predicted (Fischer, 1989):

$$T_{Cri,M} = 10600\ K \quad \text{and} \quad \rho_{Cri,M} = 1560\ kg\ m^{-3}.$$

Using the predicted critical temperature, the fitting constants in Eq. (5) are taken directly from Eq. (94), and then we obtain the critical pressure as

$$p_{Cri,M} = 157.873\ MPa.$$

Although the value of $p_{Cri,M}$ as 158 MPa was recommended by Fischer (1989), the above value is adopted hereafter for numerical consistency. Equation (94) yields a boiling point of 3811

K.

*B. Stainless steel*

Based on the theoretical vapor pressure calculated by Raoult's law, the following analytic fit is proposed for the vapor-pressure curve:

$$\log p_{Sat} = 23.47496 - \frac{22027.61}{T} + 67.2678 \times 10^{-6} T - 1.4359 \ln(T), \qquad (95)$$

where $p$ is in MPa and $T$ is in K. Using the critical temperature of iron estimated by Fortov et al. (1975), the following critical data of stainless steel are estimated assuming that the law of rectilinear diameter holds approximately:

$T_{Crt,M} = 9600$ K and $\rho_{Crt,M} = 1143$ kg m$^{-3}$.

The fitting constants in Eq. (5) are taken directly from Eq. (95), and then we obtain the critical pressure as

$p_{Crt,M} = 456.760$ MPa.

Using the above estimated critical constants, we obtain the critical compressibility of 0.280, defined by Eq. (A3) in Appendix A, which is reasonable as a liquid metal. The vapor-pressure curve calculated by Eq. (95) are shown in Fig. 1, compared with the experimental curve of type 1.4970 stainless steel determined by Bober and Singer (1985) and the theoretical curve of type 316 stainless steel evaluated by Kim (1975). Although Eq. (95) predicts about 30 % lower pressure at 4000 K than the experimental data, the difference is within the experimental uncertainty. Equation (95) yields a boiling point of 3085 K which is in good agreement with the theoretical value by Kim (1975). The heat of vaporization derived from the Clapeyron equation is 349 kJ mol$^{-1}$ at the boiling point, which is slightly lower than the experimental value by Bober and Singer (1985).

*C. Sodium*

The ANL group recommended the following vapor-pressure curve, which was determined by Browing and Potter (1985) from 864 – 2499 K:

$$\ln p_{Sat} = 11.9463 - \frac{12633.73}{T} - 0.4672 \ln T, \qquad (96)$$

where $p_{Sat}$ is in MPa, $T$ is in K. They also recommended the following critical parameters:

$T_{Crt,M} = 2503.7$ K and $\rho_{Crt,M} = 219$ kg m$^{-3}$.

Using the recommended critical temperature, the fitting constants in Eq. (5) are taken directly from Eq. (96), and then we obtain the critical pressure as

$p_{Crt,M} = 25.6406$ MPa.

Although the ANL group recommended the value of $p_{Crt,M}$ as 25.64 MPa, the above value is adopted hereafter for numerical consistency. Equation (96) yields a boiling point of 1155 K.

*4.2.2. Modified Redlich-Kwong equations*

*A. Fuel*

The specific gas constant, $R_M$, is defined from the molecular weight, $W_M$ (= $270\times10^{-3}$ kg mol$^{-1}$), as $R_M = 30.7945$ J kg$^{-1}$ K$^{-1}$. The exponent, $a_{G4,M}$, in Eq. (7) is taken from the value so as to obtain the best fit of the specific volume of saturated vapor with the theoretical data (Fischer, 1992).

Using Eq. (19) we obtain the following values:

$e_{LiqG,M} = 3.04328\times10^{6}$ J kg$^{-1}$ and $e^{D}_{LiqG,M} = 3.04329\times10^{6}$ J kg$^{-1}$ for $UO_2$, and

$e_{LiqG,M} = 2.98033\times10^{6}$ J kg$^{-1}$ and $e^{D}_{LiqG,M} = 2.98034\times10^{6}$ J kg$^{-1}$ for MOX.

The values of $c_{vG,M}$ can be calculated such that Eq. (16) satisfies the following critical internal energy by Fischer (1992):

$e_{Crt,M} = 4.9929\times10^{6}$ J kg$^{-1}$.

As the result, we obtain the following values:

$c_{vG,M} = 301.247$ J kg$^{-1}$ K$^{-1}$ for $UO_2$ and $c_{vG,M} = 306.427$ J kg$^{-1}$ K$^{-1}$ for MOX.

*B. Stainless steel*

The specific gas constant, $R_M$, is defined from the molecular weight, $W_M$ (= $55.9354\times10^{-3}$ kg mol$^{-1}$), as $R_M = 148.646$ J kg$^{-1}$ K$^{-1}$. The exponent, $a_{G4,M}$, in Eq. (7) is determined from the slope of the vapor-pressure curve, Eq. (95), at the critical temperature.

Using Eq. (19), we obtain the following values:

$e_{LiqG,M} = 7.73961\times10^{6}$ J kg$^{-1}$ and $e^{D}_{LiqG,M} = 7.73961\times10^{6}$ J kg$^{-1}$.

The value of $c_{vG,M}$ is taken from the heat capacity at constant volume of monatomic gas:

$c_{vG,M} = 1.5\,R_M = 222.969$ J kg$^{-1}$ K$^{-1}$.

As the result, the critical internal energy, $e_{Crt,M}$, is obtained by substituting the critical temperature and density into Eq. (16):

$e_{Crt,M} = 8.20580\times10^{6}$ J kg$^{-1}$.

The curve of $c_{vG,M}$ calculated by Eq. (22) along the saturation line represents that $c_{vG,M}$ gradually declines as the critical point is approached and is smaller than the monatomic gas value, $1.5\,R_M$. Although the contribution of the second term in Eq. (16) is quite small, this is an unphysical behavior brought by $a_{G4,M} < 0$. The value of $a_{G4,M}$ should be smaller than or equal to zero to fulfill the condition, $c_{vG,M} \geq 1.5\,R_M$. In addition, the MRK equation cannot describe the contribution of electronic excitation to the steel vapor energy. Assuming that steel vapor is an ideal solution of its constituents, and that vapors of these constituents behave like monatomic gas, the total energy consists of the energy of translation and of electronic excitation (Chawla et al., 1981). The translational contribution to the vapor heat capacity can be described by the monatomic gas value. Chawla et al. (1981) suggested that the electronic excitation contribution, though small at low temperature, becomes significant in a high temperature range. However, we cannot help allowing simplification assumed in the MRK equation in order to maintain the thermodynamic consistency between state variables.

*C. Sodium*

For the equilibrium constant, the following equation recommended by Golden and Tokar (1967) is used:

$$\log k_2 = -4.3249 + \frac{7204.2}{T}, \tag{97}$$

where $k_2$ is in $\text{atm}^{-1}$ and $T$ is in Rankins. This gives the EOS parameters, $d_{G1,M}$ and $d_{G2,M}$, in Eq. (12). The specific gas constant, $R_M$, is defined from the molecular weight, $W_M$ (= $22.9898\times10^{-3}$ kg $\text{mol}^{-1}$), as $R_M = 361.661$ J $\text{kg}^{-1}$ $\text{K}^{-1}$. The exponent, $a_{G4,M}$, in Eq. (9) is determined from the slope of the vapor-pressure curve, Eq. (96), at the critical temperature. From Eq. (10) we obtain the dimer fraction at the critical point as 0.540 and then the critical compressibility defined by Eq. (A26) in Appendix A becomes 0.199. This is still low, but is much closer to the usual range than the ANL value (Appendix A).

Using Eq. (19), we obtain the following values:

$$e_{LiqG,M} = 4.57699\times10^6 \text{ J kg}^{-1} \quad \text{and} \quad e^D_{LiqG,M} = 4.57844\times10^6 \text{ J kg}^{-1}.$$

From the ANL recommendation for the saturated liquid enthalpy (see Eqs. (101)), the following enthalpy is obtained at the critical temperature:

$$h_{Cri,M} = 4.29400\times10^6 \text{ J kg}^{-1}.$$

Using the critical constants determined, the critical internal energy becomes

$$e_{Cri,M} = 4.17692\times10^6 \text{ J kg}^{-1}.$$

The values of $c_{vG,M}$ can be calculated such that Eq. (18) satisfies the above critical internal

energy:

$c_{vG,M} = 460.613\ \mathrm{J\ kg^{-1}\ K^{-1}}$.

In the present study, we adopted the critical constants, $T_{Crt,M}$, $\rho_{Crt,M}$ and $h_{Crt,M}$, evaluated by the ANL group. The critical temperature was from the experimental critical pressure and Eq. (96) fitted by the experimental vapor-pressure data from 864 – 2499 K, and the critical density was determined using the critical temperature in the fits to the experimental density data from the melting point to 2200 K. The critical enthalpy is not an experimental value, but is the result of the extrapolation of the average of the liquid and vapor enthalpies using the law of rectilinear diameters. On the other hand, we can evaluate the critical internal energy from the MRK equation, Eq. (18), assuming that the heat capacity at constant volume for the dilute gas is the monatomic gas value. The resulting value, $4.35154\times10^{6}\ \mathrm{J\ kg^{-1}}$, of critical internal energy is larger than a value deduced by the ANL group. Near the critical temperature, however, the uncertainty of the liquid enthalpy recommended by the ANL group was estimated as 12 %. In view of these facts, the adopted value of critical internal energy seems to be sufficiently within the limit of the uncertainty range.

Figure 2 indicates the curves of $c_{v,Gm}$ and $c_{p,Gm}$ along the saturation line as a function of temperature. In this figure, the curves of $c_{v,Gm}$ and $c_{p,Gm}$ are calculated by Eqs. (24) and (25), respectively, and circles and triangles indicate the ANL data. The curves and the ANL data are compatible over most of the liquid temperature range. The only significant difference with the ANL data is near the critical point, where the extended MRK equation gives the finite value of $c_{v,Gm}$. Figure 3 shows the specific enthalpies of the liquid and vapor states along the saturation, evaluated using the relation, $h = e + pv$, as a function of temperature in comparison with the ANL data. As shown in Fig. 3, however, the vapor enthalpy, which is an integral quantity, agrees satisfactorily with the ANL data. It is clear that the MRK equation for a reacting system provides an improved description of the thermodynamic state of sodium vapor, which cannot be obtained by a single-component EOS.

### *4.3. Liquid properties*

#### *4.3.1. Saturated liquid*

*A. Fuel*

The following analytical fit for the saturation temperature of $UO_2$ was evaluated as a function of the liquid density (Fischer, 1992):

$$T_{Sat} = 3120 + \frac{1}{0.916\times10^{-3}}(8.86-\rho_l) - 1.7(8.86-\rho_l)^2,$$

$$2.54 < \rho_l < 8.86 \text{ g cm}^{-3} \ (T_m < T_{Sat} < 9951.66 \text{ K}), \text{ and} \quad (98a)$$

$$T_{Sat} = 10600 - 427.13(\rho_l - 1.56)^2 - 1120(\rho_l - 1.56)^3$$
$$+1242.5(\rho_l - 1.56)^4 - 365.1(\rho_l - 1.56)^5,$$

$$\rho_{Cri} < \rho_l < 2.54 \text{ g cm}^{-3} \ (9951.66 \text{ K} < T_{Sat} < T_{Cri}), \quad (98b)$$

where $T$ is in K and $\rho_l$ is in g cm$^{-3}$. For mixed oxide, to represent the difference of the melting point and density from $UO_2$, the temperature and density of $UO_2$ in the above equations are simply related to those of mixed oxide as follows:

$$T_{Sat}(\text{MOX}) = T_m(\text{MOX}) - T_m(UO_2) + T_{Sat}(UO_2), \text{ and} \quad (99a)$$

$$\rho_l(\text{MOX}) = \frac{\rho_m(\text{MOX})}{\rho_m(UO_2)} \rho_l(UO_2). \quad (99b)$$

*B. Stainless steel*

The theoretical density of type 316 stainless steel was calculated from its compositions and the densities of its constituent elements (Hull, 1969). The calculated liquid density was approximately a linear function of temperature up to 3500 K and the following equation representing a good fit to evaluated data is proposed:

$$\rho_l = 7071.4 - 0.64483(T - T_{Liq}). \quad (100)$$

where $\rho_l$ is in g kg$^{-3}$ and $T$ is in K. This linear function is used to extrapolate the liquid density up to 8000 K.

*C. Sodium*

The ANL group recommended the following melting point of sodium:

$$T_{Liq.M} = 371 \text{ K}.$$

They calculated the enthalpy of the saturated liquid sodium relative to the solid at 298.15 K by the following equations:

$$h_l = -365.77 + 1.6582T - 4.2395 \times 10^{-4}T^2 + 1.4847 \times 10^{-7}T^3 + 2992.6T^{-1},$$
$$371 \text{ K} \le T \le 2000 \text{ K}, \text{ and} \quad (101a)$$

$$h_l = E + FT - \frac{1}{2}h_{lg}, \qquad 2000 \text{ K} \le T \le 2503.7 \text{ K}, \quad (101b)$$

where $h_l$ is in kJ kg$^{-1}$, $E$ = 2128.4, $F$ = 0.86496, and $h_{lg}$ is the enthalpy of vaporization. From Eq. (101a), we obtain the specific internal energy at the melting point:

$e_{\mathrm{Liq.M}} = 2.06717 \times 10^5$ J kg$^{-1}$.

For the density of saturated liquid sodium, they recommended

$$\rho_l = \rho_{\mathrm{Crt}} + f\left(1 - \frac{T}{T_{\mathrm{Crt}}}\right) + g\left(1 - \frac{T}{T_{\mathrm{Crt}}}\right)^h, \tag{102}$$

for 371 K ≤ $T$ ≤ 2503.7 K, where $\rho_l$ is in kg m$^{-3}$, $f$ = 275.32, $g$ = 511.58, and $h$ = 0.5. Equation (102) yields the specific volume at the melting point:

$\upsilon_{\mathrm{Liq.M}} = 1.08029 \times 10^{-3}$ m$^3$ kg$^{-1}$.

As shown in Fig. 3, although the difference of enthalpies of saturated liquid and vapor between our result and the ANL data becomes large as the critical point is approached, the enthalpies evaluated using the extended MRK equation indicate the satisfactory agreement with the ANL data.

*4.3.2. Pressure derivatives*

*A. Fuel*

The following equations were recommended by Fischer (1992) as a function of density for the heat capacity at constant volume of the saturated $UO_2$ liquid:

$$c_{v,l} = 0.2925 + 0.018959(8.86 - \rho_l) - 0.0038921(8.86 - \rho_l)^2 + 0.5834 \times 10^{-4}(8.86 - \rho_l)^3,$$

$$2.54 < \rho_l < 8.86 \text{ g cm}^{-3} \ (T_m < T_{\mathrm{Sat}} < 9951.66 \text{ K}), \text{ and} \tag{103a}$$

$$c_{v,l} = 0.2597 + 0.001945(\rho_l - 1.56) + 0.010868(\rho_l - 1.56)^2,$$

$$\rho_{\mathrm{Crt}} < \rho_l < 2.54 \text{ g cm}^{-3} \ (9951.66 \text{ K} < T_{\mathrm{Sat}} < T_{\mathrm{Crt}}), \tag{103b}$$

where $c_{v,l}$ is in J g$^{-1}$ K$^{-1}$ and $\rho_l$ is in g cm$^{-3}$. Note that the original equations were discontinuous at the connecting point. We, therefore, modified the coefficients in the original equation to those appearing in Eq. (103b) so as to satisfy the continuous conditions at the connecting point. The above equations are used for $c_{v,\mathrm{Lm}}$ over the whole temperature range to calculate the pressure derivatives from Eqs. (39) and (40) for both $UO_2$ and mixed oxide. The data for mixed oxide below the melting temperature of $UO_2$ are obtained by extrapolating Eq. (103a).

Figures 4 and 5 indicate the $\alpha_{p,\mathrm{Lm}}$ by Eq. (57) and $\beta_{T,\mathrm{Lm}}$ by Eq. (50) of fuel as a function of temperature, respectively. The experimental data measured by Breitung and Reil (1990) are also shown for comparison. Excellent agreement is obtained between the present evaluation

and the Breitung and Reil's data for both $\alpha_{p,Lm}$ and $\beta_{T,Lm}$ within the uncertainty bounds.

*B. Stainless steel*

Using the speed of sound measured by Kurz and Lux (1969), Eq. (55) gives a value of $\beta_{S,Lm}$ as $8.60843\times10^{-12}$ Pa$^{-1}$ at the liquidus temperature. From this value and Eq. (51), we obtain a value of $\beta_{T,Lm}$ as $1.12435\times10^{-11}$ Pa$^{-1}$. Use of these values at the liquidus temperature yields $c_{p,Lm}$ as 782.362 J kg$^{-1}$ K$^{-1}$ from Eq. (56). The substitution of the values of $\beta_{S,Lm}$, $\beta_{T,Lm}$, and $c_{p,Lm}$ into Eq. (47) gives a value of $c_{v,Lm}$ at the liquidus temperature:

$c_{v,Lm}$ = 599.003 J kg$^{-1}$ K$^{-1}$.

We assume that $c_{v,Lm}$ is constant since this changes only little with temperature, and use the above value to calculate Eqs. (39) and (40) over the whole liquid temperature range.

*C. Sodium*

The ANL group calculated the adiabatic compressibility of liquid sodium in MPa$^{-1}$ from

$$\beta_{S,l}=\beta_{S,m}\left(1+\frac{\theta}{b}\right)\frac{1}{1-\theta}, \tag{104}$$

where the adiabatic compressibility at the melting point, $\beta_{S,m}$, is equal to $1.717\times10^{-4}$ MPa$^{-1}$, the dimensionless constant $b$ is 3.2682, and the parameter $\theta$ is defined by $\theta=\frac{T-T_m}{T_{Crt}-T_m}$.

Equation (104) is used to evaluate $c_{v,Lm}$ over the whole temperature range from Eq. (47), and then the pressure derivatives are calculated from Eqs. (39) and (40).

In Eq. (32), the partial derivative, $\left(\frac{\partial v_{Lm}}{\partial p}\right)_{e_{Lm}}$, is negative and hence the specific volume can become negative at high pressure, especially for the internal energy near the critical point. We define the bulk modulus of compressibility, $\beta_{e,Lm}$:

$$\beta_{e,Lm}=-\frac{1}{v_{Lm}}\left(\frac{\partial v_{Lm}}{\partial p}\right)_{e_{Lm}}. \tag{105}$$

Assuming the reciprocal of $\beta_{e,Lm}$, the bulk modulus of expansion, is a linear function of pressure

$$\frac{1}{\beta_{e,Lm}}=c_1+c_2p, \tag{106}$$

where $c_1$ and $c_2$ are the constants independent of pressure, and solving Eq. (105), we obtain the more general equation for liquid specific volume:

$$v_{Lm} = v_{Lm}^{+}\left\{1 - \frac{1}{\beta_M v_{Lm}^{+}}\left(\frac{\partial v_{Lm}}{\partial p}\right)_{e_{Lm}}(p - p_{Lm}^{+})\right\}^{-\beta_M}, \qquad (107)$$

where $\beta_M$ is an EOS parameter and $\beta_M = -1$ leads to Eq. (32). This approach used to derive Eq. (107) is similar to that adopted in the VENUS-II code (Jackson and Nicholson, 1972). For the case of sodium, we use a value of $\beta_M = 0.15$.

### *4.4. EOS parameters*

The method of determining the EOS parameters in thermodynamic functions is summarized as follows. The solid properties such as specific volume and internal energy were based on the available sources for oxide fuels and the new evaluation for type 316 stainless steel. The solid EOS functions were then fitted to these data by means of the least-squares method. The saturated vapor properties such as specific volume and internal energy were evaluated by the thermodynamic relationships based on the MRK equations for vapor pressure and specific internal energy and the vapor-pressure curve. The liquid-side EOS data were also evaluated consistently with the thermodynamic relations using the MRK equation on the vapor side and the Clapeyron equation. The EOS functions for the liquid and vapor states were then fitted to these evaluated data using the least-squares method. The newly evaluated EOS data of type 316 stainless steel are shown in Figs. 6 and 7 for density and specific enthalpy, respectively. A complete set of EOS parameters for uranium dioxide, mixed-oxide fuel, stainless steel, and sodium is presented in Tables 1-4. The EOS functions and parameters defined in the analytic EOS model are described in the previous chapters.

## Chapter 5. Conclusions

The analytic EOS model for the multi-phase, multi-component SIMMER–III code has been developed. Using flexible thermodynamic functions, that is, polynomial equations for the liquid and solid phases and the MRK equation for the vapor phase, the present EOS model has adequate accuracy at high temperature and high pressure and consistently satisfies basic thermodynamic relationships over a wide temperature range without deterioration of the computing efficiency. It was also proposed to extend the MRK equation to a reacting system, which describes the dimerization of sodium vapor. This was done by developing a partition function for a vapor mixture, where the vapor components obey a MRK equation. With this extended formalism, the properties of sodium can be described satisfactorily. The new scheme for pressure iteration has been also introduced into the SIMMER-III fluid-dynamics algorithm, which is fully coupled with the present EOS model. With this method, the inner EOS iteration to obtain mechanical equilibrium is eliminated by relating the cell pressure to the amount of liquid compression, and thereby the computing efficiency should be improved. The approach with a consistent overall framework developed in this study can be generally applicable to other computer codes that treat multi-phase, multi-component thermal-hydraulic phenomena.

Based on the new compilation of the most up-to-date and reliable sources available at present, the thermodynamic properties up to the critical point have been evaluated for the basic reactor-core materials: uranium dioxide, mixed-oxide fuel, stainless steel, and sodium. These EOS data completely satisfy the basic thermodynamic relationships among the EOS variables over the entire temperature ranges. It was also clarified that a few physical characteristics of properties cannot be fully described due to the simplification assumed in the analytic EOS model. However, the comparison of several properties with the available sources showed that the evaluated EOS data are thermodynamically accurate and consistent and hence appropriate for use in the analytic EOS model of SIMMER-III. It is believed that the thermodynamic properties and equations of state for the basic reactor-core materials developed in this study can be utilized as a standard data basis for the fast reactor safety analysis.

## Acknowledgments

The initial stage of this study was jointly performed under the agreement between the United States Nuclear Regulatory Commission and the Japan Nuclear Cycle Development Institute (JNC), which was formerly called the Power Reactor and Nuclear Fuel Development Corporation (PNC). The authors are grateful to W.R. Bohl of the Los Alamos National Laboratory for his significant contribution to forming the basis of SIMMER-III. Thanks are due to J.K. Fink of ANL for providing the authors with valuable information on the properties of mixed oxide. The authors would also like to acknowledge the helpful discussions with D. J. Brear, who was the International Fellow of PNC, and N. Shirakawa of Toshiba. Special thanks are due to M. Sugaya of Marubeni Software for his significant assistance in programming and computation. The present study has been completed in collaboration with FZK under the SIMMER-III code development program at JNC.

## Appendix A. MRK equation for sodium vapor EOS

### *A.1. MRK equation of state*

From Eqs. (7) and (8), the MRK pressure-volume-temperature (p–V–T) relationship is given by

$$p = \frac{R_m T}{V - b_1} - \frac{a(T)}{V(V + b_2)}, \tag{A1}$$

where $V$ is the molar volume,

$$a(T) = a_c \left( \frac{T}{T_c} \right)^{\kappa}, \qquad T < T_c, \text{ and}$$

$$a(T) = a_c + \frac{da}{dT}(T - T_c), \qquad T \geq T_c,$$

and the subscript c refers to conditions at the critical point. The MRK equation is a 4-parameter EOS and we introduce the following dimensionless parameters:

$$b_1 = b_{10} V_c, \tag{A2a}$$

$$b_2 = b_{20} V_c, \text{ and} \tag{A2b}$$

$$a = a_0 V_c R_m T_c. \tag{A2c}$$

At the critical point, Eq. (A1) can be rearranged to give an expression for the critical compressibility, $z_c$, or

$$z_c \equiv \frac{p_c V_c}{R_m T_c} = \frac{V_c}{V_c - b_1} - \frac{a_0(T_c) V_c}{V_c + b_2}. \tag{A3}$$

### *A.2. Some properties of sodium vapor*

As discussed e.g. in an early evaluation of sodium properties by Golden and Tokar (1967), there is a dimerization reaction in sodium vapor

$$2Na \leftrightarrow (Na)_2. \tag{A4}$$

In addition, Golden and Tokar assume the existence of a tetramer, which is formed by the reaction

$$4Na \leftrightarrow (Na)_4. \tag{A5}$$

They could fit experimental data better if they included the tetramer. There was, however, no experimental evidence for its existence. Neither is there any mention of a tetramer in a

Handbook article (Vargaftik and Voljak, 1985), in which sodium vapor data at temperatures up to about 1500 K are presented. The species considered in this article are the atom, the diatomic molecule, and the atomic ion plus electron. Thus, as there is a dimerization reaction in sodium vapor, one cannot expect the MRK equation, which was derived for a single-component substance, to provide a good description of the data of a mixture, which varies in composition as a function of $T$ and $V$. Furthermore, the critical compressibility of sodium, defined by Eq. (A3), is unusually low; the values quoted are 0.129 by Fink and Leibowitz (1996), and 0.123 by Thurnay (1982). For single component materials, $z_c$ is usually in the range 0.25 to 0.35. The molecular weight for the monomer was used in both evaluations. In reality the gas phase near the critical point is a mixture of the monomer, the dimer, and possibly also the tetramer. The average molecular weight is therefore larger, bringing the true value of $z_c$ closer to the range where most substances are. In the following section the MRK equation will be modified to include the effect of dimerization. However, neither ions nor a hypothetical tetramer will be included. This helps to keep the equations simple and hence they can be used in accident analysis codes.

### *A.3. EOS for a reacting system of gases*

#### *A.3.1. Helmholtz free energy for a gas of a given composition*

For an ideal gas, the partition function for one mole, Z, can be written in terms of the partition function for a single molecule, $f_g$:

$$Z = \frac{f_g^N}{N!}, \tag{A6}$$

where $f_g$ is the product of the translation, rotation, and vibration partition function, and $N$ is Avogadro's number. Using Stirling's approximation, which states that $\ln N! \approx N(\ln N - 1)$ for $N >> 1$, the function is given by

$$Z \equiv \left(\frac{f_g e}{N}\right)^N. \tag{A7}$$

The function $f_g$ can be written as a function $f_{g0}$ of temperature times the molar volume:

$$f_g = f_{g0} V. \tag{A8}$$

The statistical analogue for the Helmholtz free energy, which is defined by $F \equiv E - TS$, is

$$F(T,V) \equiv -k_B T \ln Z. \tag{A9}$$

The Helmholtz free energy for a dilute gas is then

$$F(T,V) = -Nk_B T\left(\ln\frac{f_g}{N} + 1\right). \tag{A10}$$

The above expression can be extended to the case of a real gas which obeys the MRK equation (A1) using thermodynamic relationships:

$$F(T,V) = -Nk_B T\left[\ln\frac{f_{g0}(V-b_1)}{N} + 1\right] - \frac{a}{b_2}\ln\left(1+\frac{b_2}{V}\right). \tag{A11}$$

To extend Eq. (A11) to a mixture of gases, let the mixture contain $n_i$ moles of the component i, in total

$$n_T = \sum_i n_i, \tag{A12}$$

moles. The mole fractions are then $y_i = n_i/n_T$. For the coefficients of the MRK equation, assume the following simple mixing rules:

$$b_1 = \sum_i y_i b_{1i}, \tag{A13a}$$

$$b_2 = \sum_i y_i b_{2i}, \tag{A13b}$$

$$a = \sum_i \sum_j y_i y_j a_{ij}, \tag{A13c}$$

where $a_{ij} = a_{ji}$. The Helmholtz free energy for the mixture is then expressed by

$$F(T,V,n_1,\cdots) = -R_m T\sum_i n_i\left[\ln\frac{f_{i0}(V-b_1)}{Ny_i} + 1\right] - \frac{n_T a}{b_2}\ln\left(1+\frac{b_2}{V}\right). \tag{A14}$$

From this equation, one finds easily that the pressure for the mixture is

$$p = -\left(\frac{\partial F}{\partial V}\right)_{T,n_i} = \frac{R_m T}{V-b_1} - \frac{a}{V(V+b_2)}, \text{ and} \tag{A15}$$

The chemical potentials can also be derived from Eq. (A14)

$$\mu_i = \left(\frac{\partial F}{\partial n_i}\right)_{T,V,n_j} = R_m T\left[-\ln\frac{f_{i0}(V-b_1)}{Ny_i} + \frac{b_{1i}}{V-b_1}\right]$$

$$+\left(\frac{ab_{2i}}{b_2^2} - \frac{2\sum_j y_j a_{ij}}{b_2}\right)\ln\left(1+\frac{b_2}{V}\right) - \frac{ab_{2i}}{b_2(V+b_2)}. \tag{A16}$$

*A.3.2. Extension to a gas with a dimerization reaction*

Let the mixture consist of monomer, labeled A, and dimer, B. The Helmholtz free energy is again given by Eq. (A14) and then the equilibrium condition is

$$2\mu_A = \mu_B, \tag{A17}$$

where the $\mu$ 's are given by Eq. (A16). This condition reads

$$R_m T\left[-\ln\frac{f_{A0}^{\,2} y_B (V-b_1)}{N f_{B0} y_A^{\,2}} + \frac{2b_{1A}-b_{1B}}{V-b_1}\right] + \left(\frac{a(2b_{2A}-b_{2B})}{b_2^{\,2}} - \frac{2\sum_j y_j(2a_{Aj}-a_{Bj})}{b_2}\right)\ln\left(1+\frac{b_2}{V}\right) - \frac{a(2b_{2A}-b_{2B})}{b_2(V+b_2)} = 0. \tag{A18}$$

This equation is rather complex, and in general it can be solved only numerically for $y_A$ and $y_B$. To arrive at an equation that can be fitted to known critical parameters, and can be handled in a simple way for use in hydrodynamics codes, the following simplifying assumptions will be made, which are not based on physics arguments:

$$b_{1B} = 2b_{1A}, \tag{A19a}$$

$$b_{2B} = 2b_{2A}, \text{ and} \tag{A19b}$$

$$a_{BB} = 2a_{AB} = 2a_{BA} = 4a_{AA}. \tag{A19c}$$

Then, the equilibrium condition (A18) reduces to the first term, which means that it is a quadratic equation for $y_A$ and $y_B$:

$$\frac{f_{A0}^{\,2} y_B (V-b_1)}{N f_{B0} y_A^{\,2}} = 1. \tag{A20}$$

We introduce the average molecular weight $\overline{W} = W_A(1+y_B)$ and the specific volume $\upsilon$ by the relation $V = \overline{W}\upsilon$. Furthermore, we introduce the parameters $\tilde{b}_1$, $\tilde{b}_2$ which have the dimension of a specific volume

$$b_1 = (1+y_B)b_{1A} = W_A(1+y_B)\tilde{b}_1, \text{ and} \tag{A21a}$$

$$b_2 = (1+y_B)b_{2A} = W_A(1+y_B)\tilde{b}_2. \tag{A21b}$$

In addition we have a parameter

$$a = (1+y_B)^2 a_{AA} = W_A^{\,2}(1+y_B)^2\tilde{a}. \tag{A21c}$$

Equation (A15) for the pressure can then be written

$$p=\frac{R_m T}{W_A(1+y_B)(v-\tilde{b}_1)}-\frac{\tilde{a}}{v(v+\tilde{b}_2)}. \tag{A22}$$

At the critical point, there is an inflection point in the $p-v$ curve, so that the first and the second derivatives must be zero. To evaluate $p$ at the critical point we introduce the dimensionless parameters $a_0$, $b_{10}$, and $b_{20}$

$$\tilde{b}_1=b_{10}v_c, \tag{A23a}$$

$$\tilde{b}_2=b_{20}v_c, \text{ and} \tag{A23b}$$

$$\tilde{a}=\frac{a_0 v_c R_m T_c}{W_A(1+y_{B,c})}, \tag{A23c}$$

where $v_c$ is the specific volume at the critical point and $y_{B,c}$ is the mole fraction of the dimer at the critical point. We then obtain

$$p_c=\frac{R_m T_c}{W_A(1+y_{B,c})v_c}\left(\frac{1}{1-b_{10}}-\frac{a_0}{1+b_{20}}\right). \tag{A24}$$

The gas constant per unit mass of the mixture at the critical point is

$$R_{M,c}=\frac{R_m}{W_A(1+y_{B,c})}. \tag{A25}$$

Thus, one has the critical compressibility

$$z_c=\frac{p_c v_c}{R_{M,c}T_c}=\frac{1}{1-b_{10}}-\frac{a_0}{1+b_{20}}. \tag{A26}$$

The parameters can then be determined from the known critical data of sodium as described in Section 4.2.

*A.4. Equilibrium constant*

In the literature one usually finds the equilibrium constant for the dimerization reaction (Golden and Tokar, 1967; Vargaftik and Voljak, 1985) at low pressure (ideal gas regime), which is defined as

$$k_2=\frac{y_B}{(1-y_B)^2 p_{at}}, \tag{A27}$$

where $k_2$ is in $atm^{-1}$ and $p_{at}$ is the pressure in atm. The equilibrium constant is either calculated from basic molecular parameters, or obtained from experiment. One finds from the equilibrium condition, Eq. (A20), the following relation

$$\frac{y_B}{(1-y_B)^2} = \frac{f_{B0}N}{f_{A0}^2 W_A (1+y_B)(\upsilon - \tilde{b}_1)}, \tag{A28}$$

This equation is, according to its derivation, valid for any temperature and specific volume, and can be used to extrapolate the monomer/dimer equilibrium to the critical point. We note that according to Eq. (A8) the ratio $f_{B0}N/f_{A0}^2$ is a function of temperature only. To express this ratio by the equilibrium constant, we have to specialize Eq. (A28) to the case where the ideal gas law holds. Then, the left hand side of Eq. (A28) is equal to the product of $k_2$ and the pressure $p_{at}$. Making use of this equality and applying the ideal gas law, one finds

$$\frac{f_{B0}N}{f_{A0}^2} = k_2 R_{at} T, \tag{A29}$$

where the gas constant $R_{at}$ is in atm $m^{-3}$ $mol^{-1}$ $K^{-1}$ because $k_2$ is in $atm^{-1}$. Assuming the MRK equation with the simplification by Eqs. (A19) is valid for any pressure, the equilibrium condition Eq. (A28) becomes as follows in terms of $k_2$:

$$\frac{y_B(1+y_B)}{(1-y_B)^2} = \frac{k_2 R_{at} T}{W_A(\upsilon - \tilde{b}_1)}. \tag{A30}$$

The above equation is a quadratic function of $y_B$ with a solution

$$y_B = \frac{1+2x-\sqrt{1+8x}}{2(x-1)}, \tag{A31}$$

where $x$ is the right side of Eq. (A30).

## Appendix B. Simplified analytic EOS model

### *B.1. Assumptions used in simplified analytic EOS model*

On the stage of the assessment study of the code, the thermodynamic properties of experimental materials such as water, nitrogen and organic compounds are often required for experimental analyses. Since temperature change is not large, in most of cases, the properties only over a narrow temperature range are sufficient for calculating the problems. Further, when insufficient property data are available for a material, it is difficult to prepare a complete set of the EOS parameters in the standard EOS model. Therefore, we prepare a simplified analytic EOS (SAEOS) model, which is similar to that adopted in AFDM (Henneges and Kleinheins, 1994), but is slightly improved on thermodynamic consistency.

The SAEOS model assumes simple EOS relationships: ideal gas equation, temperature-independent particle and liquid compressibilities, temperature-independent solid and liquid densities, and constant solid and liquid heat capacities. The following assumptions are used: (1) The densities of structure, particle on the sublimation curve, and saturated liquid are input constants; (2) their internal energies are assumed to depend only on temperature with constant heat capacities; (3) for solid components, the heat of fusion is given by the difference between the solidus and liquidus energies, which are the input constants; (4) for particles and liquids, the compressibilities are assumed, which are determined by constant speeds of sound; (5) vapor-pressure relationship is based on integrating the Clausius-Clapeyron equation; (6) the vapor heat capacities are constants; and (7) material dependent gas constants are used to relate partial pressures, densities, and a mixture vapor temperature. There are two differences from the AFDM-SAEOS model. First, particle and liquid densities are independent on their temperatures, but pressure-dependent compression resulting from higher cell pressure is assumed. Second, an inconsistent density dependence in the vapor internal energy is removed even if we independently assign the values to the specific gas constant and the heat capacities for vapor and liquid. This means that temperature-dependent heat of vaporization is allowed.

### *B.2. Simplified analytic EOS functions for solid properties*

The specific internal energy of structure is given by

$$e_{Sm} = c_{vS,M} T_{Sm}, \tag{B1}$$

and hence the solidus energy is defined by

$$e_{Sol,M} = c_{vS,M} T_{Sol,M}, \tag{B2}$$

where $c_{vS,M}$ is the constant heat capacity of solid. The structure temperature as a function of specific internal energy is

$$T_{Sm} = \frac{e_{Sm}}{c_{vS,M}}. \tag{B3}$$

The structure microscopic density is assumed to be constant, or

$$\upsilon_{Sm} = const. \tag{B4}$$

For particles, we neglect the temperature dependence of the particle compressibility, and approximate the compressibility of the specific volume using the constant speed of sound in the liquid state:

$$T_{Lm} = T_{Lm}^{+}, \text{ and} \tag{B5}$$

$$\upsilon_{Lm} = \upsilon_{Lm}^{+} + \left(\frac{\partial \upsilon_{Lm}}{\partial p}\right)_{M}^{o} p, \tag{B6}$$

where

$$\left(\frac{\partial \upsilon_{Lm}}{\partial p}\right)_{M}^{o} = -\left(\frac{\upsilon_{Lm}}{v_{S,Lm}}\right)^{2}, \tag{B7}$$

The right hand side of Eq. (B6) is also used for the liquid compressibility.

*B.3. Simplified analytic EOS functions for vapor properties*

*B.3.1. Vapor pressure*

The vapor obeys the ideal gas law:

$$p_{Gm} = \frac{R_M T_G}{\upsilon_{Gm}}. \tag{B8}$$

To obtain an expression for the vapor-pressure curve, we start with the Clapeyron equation, (21). By making the Clausius approximations of assuming the vapor obeys the ideal gas law and neglecting the liquid volume, Eq. (21) becomes the Clausius-Clapeyron equation

$$\left(\frac{dp}{dT}\right)_{Sat} = \frac{h_{lg} p_{Sat}}{R_M T_{Sat}^{\ 2}}. \tag{B9}$$

Assuming constant heat capacities, the heat of vaporization is given by

$$\begin{aligned} h_{lg} &= h_{lg,ref} + \int_{T_{ref}}^{T_{Sat}} (c_{v,Gm} + R_M - c_{p,Lm}) dT \\ &= h_{lg,ref} + (c_{v,Gm} + R_M - c_{p,Lm})(T_{Sat} - T_{ref}), \end{aligned} \tag{B10}$$

where $T_{ref}$ is a suitably chosen reference temperature. Equation (B10) shows the heat of

vaporization has a linear temperature dependence. Equation. (B9) may be rearranged and integrated as

$$\ln\left(\frac{p_{\mathrm{Sat}}}{p_{\mathrm{ref}}}\right)=A\left(\frac{1}{T_{\mathrm{ref}}}-\frac{1}{T_{\mathrm{Sat}}}\right)+B\ln\left(\frac{T_{\mathrm{Sat}}}{T_{\mathrm{ref}}}\right), \tag{B11}$$

where

$$A=\frac{1}{R_{\mathrm{M}}}\left[h_{\mathrm{lg,ref}}-(c_{\mathrm{v,Gm}}+R_{\mathrm{M}}-c_{\mathrm{p,Lm}})T_{\mathrm{ref}}\right], \text{ and} \tag{B12}$$

$$B=\frac{1}{R_{\mathrm{M}}}(c_{\mathrm{v,Gm}}+R_{\mathrm{M}}-c_{\mathrm{p,Lm}}). \tag{B13}$$

Equation (B11) is the three-parameter vapor-pressure expression. Assuming the constant heat of vaporization, $h_{\mathrm{lg,M}}$, or

$$c_{\mathrm{v,Gm}}+R_{\mathrm{M}}-c_{\mathrm{p,Lm}}=0, \tag{B14}$$

Eq. (B11) is approximated by the two-parameter equation:

$$\ln p_{\mathrm{Sat}}=-\frac{h_{\mathrm{lg,M}}}{R_{\mathrm{M}}T_{\mathrm{Sat}}}+\ln p_{\mathrm{M}}^{*}, \tag{B15}$$

where $\ln p_{\mathrm{M}}^{*}$ is the constant of integration. Eq. (B15) can be written as

$$p_{\mathrm{Sat}}=p_{\mathrm{M}}^{*}\exp\left(-\frac{T_{\mathrm{M}}^{*}}{T_{\mathrm{Sat}}}\right), \tag{B16}$$

where $T_{\mathrm{M}}^{*}=\frac{h_{\mathrm{lg,M}}}{R_{\mathrm{M}}}$. Although Eq. (B14) does not represent the fact that $c_{\mathrm{v,Gm}}$ and $c_{\mathrm{p,Lm}}$ can be significantly different for the material of interest, such as water at its boiling point, the error by Eq. (B15) instead of Eq. (B11) is small, if the Eq. (B15) is used only in a small temperature range and the reference temperature is chosen in the range of interest.

In the SAEOS, from Eq. (B16), the liquid vapor pressure is expressed by

$$p_{\mathrm{Lm}}^{+}=p_{\mathrm{M}}^{*}\exp\left(-\frac{T_{\mathrm{M}}^{*}}{T_{\mathrm{Lm}}^{+}}\right). \tag{B17}$$

To obtain an expression for the saturation temperature, the saturation temperature is determined from Eq. (B16),

$$T_{\mathrm{Sat,Gm}}=-\frac{T_{\mathrm{M}}^{*}}{\ln\left(\frac{p_{\mathrm{Gm}}}{p_{\mathrm{M}}^{*}}\right)}. \tag{B18}$$

*B.3.2. Vapor internal energy*

To find the equation for the specific internal energy of vapor, $e_{Gm}$, we note that the thermodynamic relation, Eq. (15), implies that $e_{Gm}$ for an ideal gas is independent of vapor density. As the result, we obtain the following equation:

$$e_{Gm} = e_{LiqG,M} + c_{vG,M}(T_G - T_{Liq,M}), \tag{B19}$$

where $e_{LiqG,M}$ is the specific internal energy of vapor at the liquidus temperature. Eq. (B19) is the thermodynamically consistent definition of vapor internal energy. Note that the vapor internal energy in AFDM (Henneges and Kleinheins, 1994) is given by the deviation from saturation condition and leads an inconsistent density dependence in the vapor internal energy unless Eq. (B14) is satisfied. Applying Eq. (B19) to $T_G = T_{Liq,M}$, we obtain

$$e_{LiqG,M} = e_{Liq,M} + h_{lg,Liq} - p_{Liq,M}(\upsilon_{LiqG,M} - \upsilon_{Liq,M}), \tag{B20}$$

where $h_{lg,Liq}$ is the heat of vaporization at the liquidus temperature. Neglecting the liquid volume and using the ideal gas law, Eq. (B8), Eq. (B20) becomes

$$e_{LiqG,M} = e_{Liq,M} + h_{lg,Liq} - R_M T_{Liq,M}. \tag{B21}$$

Therefore, the equation for the specific internal energy of vapor is expressed by

$$e_{Gm} = e_{Liq,M} + h_{lg,Liq} - R_M T_{Liq,M} + c_{vG,M}(T_G - T_{Liq,M}). \tag{B22}$$

*B.3.3. Saturated vapor*

The vapor obeys the ideal gas law and hence the specific volume of saturated vapor, or vaporization volume, satisfies the following equation:

$$p_{Gm}\upsilon_{Vap,Gm} = R_M T_{Sat,Gm}. \tag{B23}$$

Substituting Eq. (B18) to Eq. (B23), we obtain $\upsilon_{Vap,Gm}$ as a function of temperature:

$$\upsilon_{Vap,Gm} = \frac{R_M T_{Sat,Gm}}{p_M^*} \exp\left(\frac{T_M^*}{T_{Sat,Gm}}\right). \tag{B24}$$

For the specific internal energy of saturated vapor, or, vaporization energy, Eq. (B22) holds on the saturated vapor:

$$e_{Vap,Gm} = e_{Liq,M} + h_{lg,Liq} - R_M T_{Liq,M} + c_{vG,M}(T_{Sat,Gm} - T_{Liq,M}). \tag{B25}$$

### *B.4. Simplified analytic EOS functions for liquid properties*

#### *B.4.1. Saturated liquid*

The microscopic density of saturated liquid is assumed to be constant, or

$$\upsilon_{\mathrm{Con,Gm}} = const. \tag{B26}$$

The condensate energy, defined as the specific internal energy of saturated liquid, is given by

$$e_{\mathrm{Con,Gm}} = e_{\mathrm{Liq,M}} + c_{\mathrm{vL,M}}(T_{\mathrm{Sat,Gm}} - T_{\mathrm{Liq,M}}). \tag{B27}$$

where $c_{\mathrm{vL,M}}$ is the constant heat capacity of solid and the liquidus energy is defined by

$$\begin{aligned} e_{\mathrm{Liq,M}} &= e_{\mathrm{Sol,M}} + h_{\mathrm{f,M}} \\ &= c_{\mathrm{vL,M}} T_{\mathrm{Sol,M}} + h_{\mathrm{f,M}}. \end{aligned} \tag{B28}$$

#### *B.4.2. Compressed liquid*

We neglect the effect of compressibility on the temperature, similarly to particle:

$$T_{\mathrm{Lm}} = T^{+}_{\mathrm{Lm}} + \left(\frac{\partial T_{\mathrm{Lm}}}{\partial p}\right)_{e_{\mathrm{Lm}}} (p - p^{+}_{\mathrm{Lm}}). \tag{B29}$$

The saturated liquid temperature, $T^{+}_{\mathrm{Lm}}$, as a function of specific internal energy is expressed by

$$T^{+}_{\mathrm{Lm}} = T_{\mathrm{Liq,M}} + \frac{e_{\mathrm{Lm}} - e_{\mathrm{Liq,M}}}{c_{\mathrm{vL,M}}}. \tag{B30}$$

For the liquid specific volume, the constant liquid compressibility is assumed and the compressibility of the specific volume is approximated by the speed of sound in the liquid state:

$$\upsilon_{\mathrm{Lm}} = \upsilon^{+}_{\mathrm{Lm}} + \left(\frac{\partial \upsilon_{\mathrm{Lm}}}{\partial p}\right)_{e_{\mathrm{Lm}}} (p - p^{+}_{\mathrm{Lm}}), \tag{B31}$$

where

$$\upsilon^{+}_{\mathrm{Lm}} = const., \text{ and} \tag{B32}$$

$$\left(\frac{\partial \upsilon_{\mathrm{Lm}}}{\partial p}\right)_{e_{\mathrm{Lm}}} \approx -\upsilon_{\mathrm{Lm}} \beta_{\mathrm{S,Lm}} = -\left(\frac{\upsilon_{\mathrm{Liq,M}}}{v_{\mathrm{S,Lm}}}\right)^2. \tag{B33}$$

## Appendix C. Nomenclature

| | |
|---|---|
| $c_{Sat}$ | heat capacity along a saturation curve (J kg$^{-1}$ K$^{-1}$) |
| $c_p$, $c_v$ | heat capacities at constant pressure, constant volume (J kg$^{-1}$ K$^{-1}$) |
| $E$ | molar internal energy (J mol$^{-1}$) |
| $e$ | specific internal energy (J kg$^{-1}$) |
| $F$ | molar Helmholtz free energy (J mol$^{-1}$) |
| $f_g$ | partition function for a single molecule |
| $h$ | specific enthalpy (J kg$^{-1}$) |
| $h_f$ | heat of fusion (J kg$^{-1}$) |
| $h_{lg}$ | heat of vaporization (J kg$^{-1}$) |
| $k_2$ | equilibrium constant (Pa$^{-1}$ or atm$^{-1}$) |
| $k_B$ | Boltzmann's constant (J K$^{-1}$) |
| $N$ | Avogadro's number |
| $n$ | number of moles |
| $p$ | pressure (Pa) |
| $p_{at}$ | pressure (atm) |
| $R$ | gas constant (J kg$^{-1}$ K$^{-1}$) |
| $R_m$ | gas constant (J mol$^{-1}$ K$^{-1}$) |
| $R_{at}$ | gas constant (atm m$^{-3}$ mol$^{-1}$ K$^{-1}$) |
| $T$ | temperature (K) |
| $S$ | specific entropy (J kg$^{-1}$) |
| $V$ | molar volume (m$^3$ mol$^{-1}$) |
| $W$ | molecular weight (kg mol$^{-1}$) |
| $y$ | mole fraction |
| $y_B$ | dimer fraction |
| $z_c$ | critical compressibility |
| $Z$ | molar partition function |

### *Greek letters*

| | |
|---|---|
| $\alpha_p$ | volumetric thermal expansion coefficient (K$^{-1}$) |
| $\beta_S$ | adiabatic compressibility (Pa$^{-1}$) |
| $\beta_T$ | isothermal compressibility (Pa$^{-1}$) |
| $v_S$ | speed of sound (m s$^{-1}$) |
| $\rho$ | density (kg m$^{-3}$) |
| $\overline{\rho}$ | macroscopic density (kg m$^{-3}$) |
| $v$ | specific volume (m$^3$ kg$^{-1}$) |
| $\mu$ | chemical potential (J mol$^{-1}$) |

### *Subscripts*

| | |
|---|---|
| A | atomic sodium (monomer) |
| B | sodium vapor molecule (dimer) |
| Con | saturated liquid |
| Crt, c | critical point |
| G | vapor mixture |
| Gm | material component m in vapor field |

| | |
|---|---|
| i, j | labels of components in a mixture |
| l | liquid state |
| Liq | liquidus point |
| LiqG | vapor at liquidus point |
| Lm | energy component m in liquid field |
| M | material number |
| m | melting point |
| s | solid state |
| Sat | saturation |
| Sm | energy component m in structure field |
| Sol | solidus point |
| T | total |
| Vap | saturated vapor |

*Superscripts*

| | |
|---|---|
| D | dilute vapor |
| + | lack of pressure dependence |

## References


Adamson, M.G., Aitken, E.A., Caputi, R.W., 1985. Experimental and thermodynamic evaluation of the melting behavior of irradiated oxide fuels, J. Nucl. Mater. 130, 349–365.

Belton, G.R., Fruehan, R.J., 1970. Mass-spectrometric determination of activities in Fe-Cr and Fe-Cr-Ni alloys, Metallurgical Transactions 1, 781–787.

Bober, M., Singer, J., 1985. High temperature vapor pressures of metals from laser evaporation, High Temperature Science 19, 329–345.

Bober, M., Singer, J., 1987. Vapor pressure determination of liquid $UO_2$ using a boiling point technique, Nucl. Sci. Eng. 97, 344–352.

Bohl, W.R., Luck, L.B., 1990. SIMMER-II: A computer program for LMFBR disrupted core analysis, LA-11415-MS, Los Alamos National Laboratory, June 1990.

Bohl, W.R., Wilhelm, D., Parker, F.R., Berthier, J., Goutagny, L., Ninokata, H., 1990. AFDM: An advanced fluid-dynamics model, Volume I: Scope, approach, and summary, LA-11692-MS, Vol. I, Los Alamos National Laboratory, September 1990.

Breitung, W., Reil, K.O., 1989. Vapor pressure measurements on liquid uranium oxide and (U, Pu) mixed oxide, Nucl. Sci. Eng. 101, 26–40.

Breitung, W., Reil, K.O., 1990. The density and compressibility of liquid (U, Pu)-mixed oxide, Nucl. Sci. Eng. 105, 205–217.

Chawla, T.C., Graff, D.L., Borg, R.C., Bordner, G.L., Weber, D.P., Millaer, D., 1981. Thermophysical properties of mixed oxide fuel and stainless steel type 316 for use in transition phase analysis, Nucl. Eng. Des. 67, 57–74.

Carey, V.P., 1992. Liquid-Vapor Phase-Change Phenomena: An Introduction to the Thermophysics of Vaporization and Condensation Processes in Heat Transfer Equipment, Hemisphere Pub. Corp., Washington.

Drotning, W.D., 1982. Thermal expansion of molten uranium dioxide. In Sengers, J.V. (Ed.), Proceedings of the Eighth Symposium on Thermophysical Properties Vol. II: Thermophysical properties of solid and of selected fluids for energy technology, ASME, New York, pp. 245–249.

Fink, J.K., Leibowitz, L., 1982. Calculation of thermophysical properties of sodium. In Sengers, J.V. (Ed.), Proceedings of the Eighth Symposium on Thermophysical Properties Vol. II: Thermophysical properties of solid and of selected fluids for energy technology, ASME, New York, pp. 165–173.

Fink, J.K., Leibowitz, L., 1995. Thermodynamic and Transport Properties of Sodium Liquid and Vapor, ANL/RE-95/2, Argonne National Laboratory, January 1995.

Fink, J.K., Leibowitz, L., 1996. A consistent assessment of the thermophysical properties of sodium, High Temp. Mater. Sci. 35, 65–103.

Fink, J.K., Petri, M.C., 1997. Thermophysical Properties of Uranium Dioxide, ANL/RE-97/2, Argonne National Laboratory, February 1997.

Fischer, E.A., 1987. Evaluation of the urania equation of state based on recent vapour pressure measurements, KfK 4084, Kernforschungszentrum Karlsruhe, September 1987.

Fischer, E.A., 1989. A new evaluation of the urania equation of state based on recent vapor pressure, Nucl. Sci. Eng. 101, 97–116.

Fischer, E.A., 1992. Fuel equation of state data for use in fast reactor accident analysis codes, KfK 4889, Kernforschungszentrum Karlsruhe, May 1992.

Fortov, V.E., Dremin, A.N., Leont'ev, A.A., 1975. Evaluation of the parameters of the critical point, High Temperature, 13, 984–992.

Golden, G.H., Tokar, J.V., 1967. Thermophysical properties of sodium, ANL-7323, Argonne National Laboratory, August 1967.

Grosse, A.V., 1971. Simple empirical relationship between the compressibility of ideal liquids and temperature up to the critical point, Nature Physical Science 232, 170–171.

Harding, J.H., Martin, D.G., Potter, P.E., 1989. Thermophysical and thermodynamic properties of fast reactor materials, Commission of the European Communities, EUR 12402 EN.

Henneges, G., Kleinheins, S., 1994. AFDM: An advanced fluid-dynamics model, Volume VI: EOS-AFDM interface, LA-11692-MS, Vol. VI, Los Alamos National Laboratory, January 1994.

Hull, F.C., 1969. Estimating alloy densities, Metal Progress 96, 139–140.

Kim, C.S., 1975. Thermophysical properties of stainless steel, ANL-75-55, Argonne National Laboratory, September 1975.

Kondo, Sa., Tobita, Y., Morita, K., Shirakawa, N., 1992. SIMMER-III: An advanced computer program for LMFBR severe accident analysis, Proceedings of the International Conference on Design and Safety of Advanced Nuclear Power Plant (ANP '92), Vol. IV, Tokyo, Japan, 25–29 October, 1992, pp. 40.5-1–40.5-11.

Kurz, W., Lux, B., 1969. Die Schallgeschwindigkeit von Eisen und Eisenlegierungen im festen und flüssigen Zustand, High Temperatures - High Pressures 1, 387–399.

Jackson, J.F., Nicholson, R.B., 1972. VENUS-II: An LMFBR disassembly program, ANL-7951, Argonne National Laboratory, September 1972.

Limon, R., Sutren, G., Combette, P., Barbry, F., 1981. Equation of sate of non irradiated $UO_2$, Proceedings of the ANS/ENS Topical Meeting on Reactor Safety Aspects of Fuel Behaviour, Vol. 2, Sun Valley, Idaho, 2-6, August, 1981, pp.576–583.

Martin, D.G., 1988. The thermal expansion of solid $UO_2$ and (U,Pu) mixed oxides – A review and recommendations, J. Nucl. Mater. 152, 94–101.

Morita, K., Tobita, Y., Kondo, Sa., Shirakawa, N., Brear, D.J., 1994. Multiphase, multicomponent heat- and mass-transfer modeling in SIMMER-III, Proceeding of the International Topical Meeting on Sodium Cooled Fast Reactor Safety (FRS '94), Vol. 2, Obninsk, Russia, 3-7 October, 1994, pp. 290–299.

Ohse, R.W., Babelot, J.F., Cercignani, C., Hiernaut, J.P., Hoch, M., Hyland, G.J., Magill, J., 1985. Equation of state of uranium oxide, J. Nucl. Mater. 130, 165–179.

Rand, M.H., Ackermann, R.J., Grønvold, F., Oetting, F.L., Pattoret, A., 1978. The thermodynamic properties of the urania phase, Rev. int. hautes Tempér. Réfract. Fr. 15, 355–365.

Redlich, O., Kwong, J.N.S., 1949. On the Thermodynamics of solutions. V, An equation of state. Fugacities of gaseous solutions, Chem. Rev. 44, 233-244.

Riedel, L. 1982. 1954. Eine neue universelle Dampfdruckformel, Chemie-Ing.-Techn. 26, 83–89.

Rowlinson, J.S., Swinton, F.L., 1982. Liquids and Liquid Mixtures, 3rd Ed., Butterworth & Co. Ltd., London.

Saul, A., Wanger, W., 1987. International equations for the saturation properties of ordinary water substance, J. Phys. Chem. Ref. Data 16, 893–901.

Thurnay, K., 1982. Evaluation of thermophysical properties of sodium as surfaces of the temperature and the density, Nucl. Sci. Eng. 82, 181–189.

Vargaftik, N.B., Voljak, L.D., 1985. Thermodynamic properties of alkali metal vapours at low pressures. In: Ohse, R.W. (Ed.), Handbook of Thermodynamic and Transport Properties of Alkali Metals, Chapter 6.6, Blackwell Scientific Publications, Oxford, pp. 535–576.

Table 1. EOS parameters for $UO_2$.

| | | |
|---|---|---|
| $e_{Sol} = 1.12157\times10^{6}$ | $T_{Sol} = 3.12000\times10^{3}$ | $v_{Sol} = 1.03620\times10^{-4}$ |
| $e_{Liq} = 1.39871\times10^{6}$ | $T_{Liq} = 3.12000\times10^{3}$ | $v_{Liq} = 1.12867\times10^{-4}$ |
| $e_{Crt} = 4.99290\times10^{6}$ | $T_{Crt} = 1.06000\times10^{4}$ | $\rho_{Crt} = 1.56000\times10^{3}$ |
| $p_{Crt} = 1.57873\times10^{8}$ | $e_{LiqG} = 3.04328\times10^{6}$ | $e^{D}_{LiqG} = 3.04329\times10^{6}$ |
| $c_{vG} = 3.01247\times10^{2}$ | $R = 3.07945\times10$ | $W = 2.70000\times10^{-1}$ |
| $a_{S1} = 4.44390\times10^{-1}$ | $a_{S2} = 4.89576\times10^{-1}$ | $a_{S3} = -2.83438\times10^{-2}$ |
| $b_{S1} = -1.00628\times10^{-1}$ | $b_{S2} = -7.86430\times10^{-2}$ | $b_{S3} = 5.84342\times10^{-2}$ |
| $a_{L1} = 8.81083\times10^{-1}$ | $a_{L2} = -2.04486\times10^{-2}$ | $a_{L3} = 1.86174\times10^{-2}$ |
| $a_{L4} = 3.47820$ | $a_{L5} = 2.95237\times10$ | $a_{L6} = -1.69116\times10^{2}$ |
| $b_{L1} = 2.17296\times10$ | $b_{L2} = 4.42327\times10^{-4}$ | $b_{L3} = -7.99342\times10^{4}$ |
| $b_{L4} = -8.88130$ | | |
| $c_{L1} = -3.51500\times10$ | $c_{L2} = 6.72600\times10$ | $c_{L3} = -4.70436\times10$ |
| $c_{L4} = 8.08263$ | | |
| $d_{L1} = 3.93703\times10^{-1}$ | $d_{L2} = -1.81812\times10^{-1}$ | $d_{L3} = 1.74487\times10^{-1}$ |
| $d_{L4} = 2.89613$ | $d_{L5} = -1.54733$ | $d_{L6} = 2.07800$ |
| $f_{L1} = -3.61402\times10^{-12}$ | $f_{L2} = -4.22202\times10^{-2}$ | $f_{L3} = -1.68215\times10$ |
| $f_{L4} = 3.17194\times10$ | $f_{L5} = -2.92392\times10$ | $f_{L6} = -1.42655\times10^{-11}$ |
| $\left(\frac{\partial T_{Lm}}{\partial p}\right)^{0} = 5.52486\times10^{-8}$ | $\left(\frac{\partial v_{Lm}}{\partial p}\right)^{0} = -5.46331\times10^{-16}$ | |
| $\left(\frac{\partial T_{Lm}}{\partial p}\right)_{e_{Crt}} = 1.91288\times10^{-5}$ | | |
| $a_{G1} = 1.41301\times10^{-4}$ | $a_{G2} = 2.94299\times10^{2}$ | $a_{G3} = 2.85846\times10^{-4}$ |
| $a_{G4} = 2.00000\times10^{-1}$ | | |
| $b_{G1} = 3.90118\times10^{-1}$ | $b_{G2} = 2.64047$ | $b_{G3} = 1.79946$ |
| $b_{G4} = 9.17799$ | $b_{G5} = 2.31365\times10$ | $b_{G6} = 6.07538\times10$ |
| $c_{G1} = 2.97266\times10^{2}$ | $c_{G2} = 2.35586\times10^{-3}$ | $c_{G3} = -8.26332\times10^{-7}$ |
| $c_{G4} = 9.69434\times10^{-1}$ | $c_{G5} = 4.22861\times10^{-4}$ | $c_{G6} = -8.11911\times10^{-8}$ |
| $d_{G1} =$ ------- | $d_{G2} =$ ------- | |
| $f_{G1} = 5.57168\times10^{-1}$ | $f_{G2} = 2.78675$ | $f_{G3} = 1.69876\times10^{-7}$ |
| $f_{G4} = -1.76528\times10^{-8}$ | | |
| $a_{Sat1} = 4.50854\times10^{-4}$ | $a_{Sat2} = -1.57919\times10^{-5}$ | $a_{Sat3} = 1.69876\times10^{-7}$ |
| $a_{Sat4} = -1.76528\times10^{-8}$ | | |
| $b_{Sat1} = -1.03384\times10^{-4}$ | $b_{Sat2} = -1.48030\times10^{-10}$ | $b_{Sat3} = -3.78342\times10^{-16}$ |
| $b_{Sat4} = 8.01887\times10^{-1}$ | $b_{Sat5} = 2.53025\times10^{-2}$ | $b_{Sat6} = 7.62684\times10^{-8}$ |
| $c_{Sat1} = 5.14152\times10^{2}$ | $c_{Sat2} = 5.84459\times10^{-4}$ | $c_{Sat3} = -8.30648\times10^{-7}$ |
| $c_{Sat4} = 9.81132\times10^{-1}$ | $c_{Sat5} = 1.91882\times10^{-3}$ | $c_{Sat6} = 2.59729\times10^{-8}$ |

Table 2. EOS parameters for MOX.

| | | |
|---|---|---|
| $e_{Sol} = 1.05162\times10^{6}$ | $T_{Sol} = 3.00200\times10^{3}$ | $v_{Sol} = 1.00230\times10^{-4}$ |
| $e_{Liq} = 1.31829\times10^{6}$ | $T_{Liq} = 3.04100\times10^{3}$ | $v_{Liq} = 1.08814\times10^{-4}$ |
| $e_{Cri} = 4.99290\times10^{6}$ | $T_{Cri} = 1.06000\times10^{4}$ | $\rho_{Cri} = 1.56000\times10^{3}$ |
| $p_{Cri} = 1.57873\times10^{8}$ | $e_{LiqG} = 2.98033\times10^{6}$ | $e^{D}_{LiqG} = 2.98034\times10^{6}$ |
| $c_{vG} = 3.06427\times10^{2}$ | $R = 3.07945\times10$ | $W = 2.70000\times10^{-1}$ |
| $a_{S1} = 4.68166\times10^{-1}$ | $a_{S2} = 5.24030\times10^{-1}$ | $a_{S3} = -9.59833\times10^{-2}$ |
| $b_{S1} = -6.48590\times10^{-3}$ | $b_{S2} = -1.62062\times10^{-1}$ | $b_{S3} = 7.27906\times10^{-2}$ |
| $a_{L1} = 8.41923\times10^{-1}$ | $a_{L2} = -1.69174\times10^{-2}$ | $a_{L3} = 1.47156\times10^{-2}$ |
| $a_{L4} = 3.68955$ | $a_{L5} = 2.89670\times10$ | $a_{L6} = -1.66741\times10^{2}$ |
| $b_{L1} = 2.17296\times10$ | $b_{L2} = 4.42327\times10^{-4}$ | $b_{L3} = -7.99342\times10^{4}$ |
| $b_{L4} = -8.88130$ | | |
| $c_{L1} = -4.16525\times10$ | $c_{L2} = 9.47848\times10$ | $c_{L3} = -7.88238\times10$ |
| $c_{L4} = 1.97832\times10$ | | |
| $d_{L1} = 3.72680\times10^{-1}$ | $d_{L2} = -1.67343\times10^{-1}$ | $d_{L3} = 1.44446\times10^{-1}$ |
| $d_{L4} = 3.06379$ | $d_{L5} = -1.55974$ | $d_{L6} = 2.09893$ |
| $f_{L1} = -1.32899\times10^{-12}$ | $f_{L2} = 1.90472\times10^{-1}$ | $f_{L3} = -1.42352\times10$ |
| $f_{L4} = 2.15440\times10$ | $f_{L5} = -1.93115\times10$ | $f_{L6} = -1.42655\times10^{-11}$ |
| $\left(\frac{\partial T_{Lm}}{\partial p}\right)^{o} = 5.85547\times10^{-8}$ | $\left(\frac{\partial v_{Lm}}{\partial p}\right)^{o} = -5.46331\times10^{-16}$ | |
| $\left(\frac{\partial T_{Lm}}{\partial p}\right)_{e_{Cri}} = 1.91288\times10^{-5}$ | | |
| $a_{G1} = 1.41301\times10^{-4}$ | $a_{G2} = 2.94299\times10^{2}$ | $a_{G3} = 2.85846\times10^{-4}$ |
| $a_{G4} = 2.00000\times10^{-1}$ | | |
| $b_{G1} = 3.90118\times10^{-1}$ | $b_{G2} = 2.64047$ | $b_{G3} = 1.79946$ |
| $b_{G4} = 9.17799$ | $b_{G5} = 2.31365\times10$ | $b_{G6} = 6.07538\times10$ |
| $c_{G1} = 3.02512\times10^{2}$ | $c_{G2} = 2.41081\times10^{-3}$ | $c_{G3} = -8.14218\times10^{-7}$ |
| $c_{G4} = 9.69623\times10^{-1}$ | $c_{G5} = 4.17946\times10^{-4}$ | $c_{G6} = -8.32298\times10^{-8}$ |
| $d_{G1} =$ -------- | $d_{G2} =$ ------- | |
| $f_{G1} = 5.57168\times10^{-1}$ | $f_{G2} = 2.78675$ | $f_{G3} = 1.85168$ |
| $f_{G4} = 1.07188\times10$ | | |
| $a_{Sat1} = 4.50854\times10^{-4}$ | $a_{Sat2} = -1.57919\times10^{-5}$ | $a_{Sat3} = 1.69876\times10^{-7}$ |
| $a_{Sat4} = -1.76528\times10^{-8}$ | | |
| $b_{Sat1} = -1.03373\times10^{-4}$ | $b_{Sat2} = -1.47509\times10^{-10}$ | $b_{Sat3} = -4.25199\times10^{-16}$ |
| $b_{Sat4} = 9.43396\times10^{-1}$ | $b_{Sat5} = 2.30701\times10^{-2}$ | $b_{Sat6} = 1.25429\times10^{-7}$ |
| $c_{Sat1} = 5.20115\times10^{2}$ | $c_{Sat2} = 4.38079\times10^{-4}$ | $c_{Sat3} = -7.99968\times10^{-7}$ |
| $c_{Sat4} = 9.81132\times10^{-1}$ | $c_{Sat5} = 1.93566\times10^{-3}$ | $c_{Sat6} = 2.74910\times10^{-8}$ |

Table 3. EOS parameters for stainless steel.

| | | |
|---|---|---|
| $e_{Sol} = 9.12379\times10^{5}$ | $T_{Sol} = 1.71300\times10^{3}$ | $v_{Sol} = 1.36168\times10^{-4}$ |
| $e_{Liq} = 1.25158\times10^{6}$ | $T_{Liq} = 1.75300\times10^{3}$ | $v_{Liq} = 1.41420\times10^{-4}$ |
| $e_{Crt} = 8.20580\times10^{6}$ | $T_{Crt} = 9.60000\times10^{3}$ | $\rho_{Crt} = 1.14300\times10^{3}$ |
| $p_{Crt} = 4.56760\times10^{8}$ | $e_{LiqG} = 7.73961\times10^{6}$ | $e^{D}_{LiqG} = 7.73961\times10^{6}$ |
| $c_{vG} = 2.22969\times10^{2}$ | $R = 1.48646\times10^{2}$ | $W = 5.59354\times10^{-2}$ |
| $a_{S1} = 8.56796\times10^{-1}$ | $a_{S2} = -3.28896\times10^{-1}$ | $a_{S3} = 2.92311\times10^{-1}$ |
| $b_{S1} = -9.08374\times10^{-2}$ | $b_{S2} = 4.23217\times10^{-2}$ | $b_{S3} = -1.96932\times10^{-2}$ |
| $a_{L1} = 1.02425$ | $a_{L2} = -6.82077\times10^{-2}$ | $a_{L3} = 6.60477\times10^{-3}$ |
| $a_{L4} = 6.00388$ | $a_{L5} = 5.95140$ | $a_{L6} = 0.00000$ |
| $b_{L1} = 2.37361\times10$ | $b_{L2} = 1.54890\times10^{-4}$ | $b_{L3} = -5.07204\times10^{4}$ |
| $b_{L4} = -3.30628$ | | |
| $c_{L1} = -9.23249$ | $c_{L2} = -1.74176\times10$ | $c_{L3} = 3.84477\times10$ |
| $c_{L4} = -1.89791\times10$ | | |
| $d_{L1} = 1.81594\times10^{-1}$ | $d_{L2} = -6.22683\times10^{-3}$ | $d_{L3} = 8.98282\times10^{-3}$ |
| $d_{L4} = 5.17704$ | $d_{L5} = -1.62972$ | $d_{L6} = 2.71165$ |
| $f_{L1} = -2.58082\times10^{-13}$ | $f_{L2} = 1.01637$ | $f_{L3} = -1.55026\times10$ |
| $f_{L4} = 4.54114\times10$ | $f_{L5} = -4.07002\times10$ | $f_{L6} = -1.01686\times10^{-12}$ |
| $\left(\frac{\partial T_{Lm}}{\partial p}\right)^{o} = 1.92381\times10^{-8}$ | $\left(\frac{\partial v_{Lm}}{\partial p}\right)^{o} = -6.58746\times10^{-16}$ | |
| $\left(\frac{\partial T_{Lm}}{\partial p}\right)_{e_{Crt}} = 6.06817\times10^{-6}$ | | |
| $a_{G1} = 1.51243\times10^{-4}$ | $a_{G2} = 2.02244\times10^{3}$ | $a_{G3} = 6.50753\times10^{-4}$ |
| $a_{G4} = 2.57346\times10^{-1}$ | | |
| $b_{G1} = -1.19877\times10^{-1}$ | $b_{G2} = 4.83281$ | $b_{G3} = -1.04117$ |
| $b_{G4} = 1.28107\times10$ | $b_{G5} = 9.77240$ | $b_{G6} = 6.14938\times10$ |
| $c_{G1} = 2.15388\times10^{2}$ | $c_{G2} = 9.04415\times10^{-3}$ | $c_{G3} = -2.83239\times10^{-6}$ |
| $c_{G4} = 8.33333\times10^{-1}$ | $c_{G5} = 2.19035\times10^{-3}$ | $c_{G6} = -8.43355\times10^{-9}$ |
| $d_{G1} = -------$ | $d_{G2} = -------$ | |
| $f_{G1} = 3.48245\times10^{-1}$ | $f_{G2} = 4.39524$ | $f_{G3} = -7.32274\times10^{-1}$ |
| $f_{G4} = 1.43431\times10$ | | |
| $a_{Sat1} = 5.77921\times10^{-4}$ | $a_{Sat2} = -2.08089\times10^{-5}$ | $a_{Sat3} = -1.61242\times10^{-8}$ |
| $a_{Sat4} = -6.56103\times10^{-9}$ | | |
| $b_{Sat1} = -9.11919\times10^{-5}$ | $b_{Sat2} = 0.00000$ | $b_{Sat3} = 0.00000$ |
| $b_{Sat4} = 8.33333\times10^{-1}$ | $b_{Sat5} = 4.03621\times10^{-2}$ | $b_{Sat6} = 1.86344\times10^{-8}$ |
| $c_{Sat1} = 6.80662\times10^{2}$ | $c_{Sat2} = 3.91671\times10^{-2}$ | $c_{Sat3} = -2.32314\times10^{-6}$ |
| $c_{Sat4} = 8.33333\times10^{-1}$ | $c_{Sat5} = 4.14974\times10^{-3}$ | $c_{Sat6} = 1.79897\times10^{-8}$ |

Table 4. EOS parameters for sodium.

| | | |
|---|---|---|
| $e_{Sol}$ = ------- | $T_{Sol}$ = ------- | $v_{Sol}$ = ------- |
| $e_{Liq}$ = 2.06717×10$^{5}$ | $T_{Liq}$ = 3.71000×10$^{2}$ | $v_{Liq}$ = 1.08029×10$^{-3}$ |
| $e_{Cri}$ = 4.17692×10$^{6}$ | $T_{Cri}$ = 2.50370×10$^{3}$ | $\rho_{Cri}$ = 2.19000×10$^{2}$ |
| $p_{Cri}$ = 2.56406×10$^{7}$ | $e_{LiqG}$ = 4.57699×10$^{6}$ | $e^{D}_{LiqG}$ = 4.57844×10$^{6}$ |
| $c_{vG}$ = 4.60613×10$^{2}$ | $R$ = 3.61661×10$^{2}$ | $W$ = 2.29898×10$^{-2}$ |
| $a_{S1}$ = ------- | $a_{S2}$ = ------- | $a_{S3}$ = ------- |
| $b_{S1}$ = ------- | $b_{S2}$ = ------- | $b_{S3}$ = ------- |
| $a_{L1}$ = 5.76094×10$^{-1}$ | $a_{L2}$ =-2.33486×10$^{-2}$ | $a_{L3}$ = 4.72888×10$^{-4}$ |
| $a_{L4}$ = 1.99989×10 | $a_{L5}$ =-1.08409×10$^{2}$ | $a_{L6}$ = 8.96169×10$^{3}$ |
| $b_{L1}$ = 2.21057×10 | $b_{L2}$ = 0.00000 | $b_{L3}$ =-1.26337×10$^{4}$ |
| $b_{L4}$ =-4.67200×10$^{-1}$ | | |
| $c_{L1}$ =-2.42195×10 | $c_{L2}$ = 2.99496×10 | $c_{L3}$ =-3.39662 |
| $c_{L4}$ =-8.16499 | | |
| $d_{L1}$ = 6.276650×10$^{-2}$ | $d_{L2}$ =-2.217050×10$^{-3}$ | $d_{L3}$ = 2.277400×10$^{-4}$ |
| $d_{L4}$ = 1.707250×10 | $d_{L5}$ =-1.267217 | $d_{L6}$ = 2.598375 |
| $f_{L1}$ =-3.09510×10$^{-12}$ | $f_{L2}$ = 5.59746×10$^{-1}$ | $f_{L3}$ =-4.64421 |
| $f_{L4}$ = 4.33770 | $f_{L5}$ =-3.36198 | $f_{L6}$ =-1.46413×10$^{-10}$ |
| $\left(\frac{\partial T_{Lm}}{\partial p}\right)^{o}$ = 9.51892×10$^{-8}$ | $\left(\frac{\partial v_{Lm}}{\partial p}\right)^{o}$ =-1.85485×10$^{-13}$ | |
| $\left(\frac{\partial T_{Lm}}{\partial p}\right)_{e_{Cri}}$ = 2.11232×10$^{-5}$ | | |
| $a_{G1}$ = 2.93447×10$^{-4}$ | $a_{G2}$ = 1.23634×10$^{4}$ | $a_{G3}$ = 1.96134×10$^{-2}$ |
| $a_{G4}$ = 4.92937×10$^{-1}$ | | |
| $b_{G1}$ = 2.42590×10$^{-1}$ | $b_{G2}$ = 7.33754 | $b_{G3}$ =-3.20191 |
| $b_{G4}$ = 1.88331×10 | $b_{G5}$ = 3.94583 | $b_{G6}$ = 7.19859×10 |
| $c_{G1}$ = 3.35053×10$^{2}$ | $c_{G2}$ =-4.36960×10$^{-1}$ | $c_{G3}$ = 1.83657×10$^{-4}$ |
| $c_{G4}$ = 6.98966×10$^{-1}$ | $c_{G5}$ = 6.74084×10$^{-3}$ | $c_{G6}$ =-1.09662×10$^{-7}$ |
| $d_{G1}$ =-2.14845×10 | $d_{G2}$ = 9.21571×10$^{3}$ | |
| $f_{G1}$ = 9.50847×10$^{-1}$ | $f_{G2}$ = 6.26498 | $f_{G3}$ = 9.88924 |
| $f_{G4}$ = 2.19575×10 | | |
| $a_{Sat1}$ = 1.80128×10$^{-3}$ | $a_{Sat2}$ =-8.05016×10$^{-5}$ | $a_{Sat3}$ = 4.82697×10$^{-8}$ |
| $a_{Sat4}$ =-8.53040×10$^{-9}$ | | |
| $b_{Sat1}$ =-2.57567×10$^{-4}$ | $b_{Sat2}$ = 3.02115×10$^{-8}$ | $b_{Sat3}$ =-2.75445×10$^{-11}$ |
| $b_{Sat4}$ = 9.18640×10$^{-1}$ | $b_{Sat5}$ = 5.35439×10$^{-2}$ | $b_{Sat6}$ = 4.88971×10$^{-8}$ |
| $c_{Sat1}$ = 9.98522×10$^{2}$ | $c_{Sat2}$ = 1.14342×10$^{-1}$ | $c_{Sat3}$ = 1.40119×10$^{-4}$ |
| $c_{Sat4}$ = 9.98522×10$^{-1}$ | $c_{Sat5}$ = 2.76460×10$^{-3}$ | $c_{Sat6}$ = 1.18490×10$^{-5}$ |

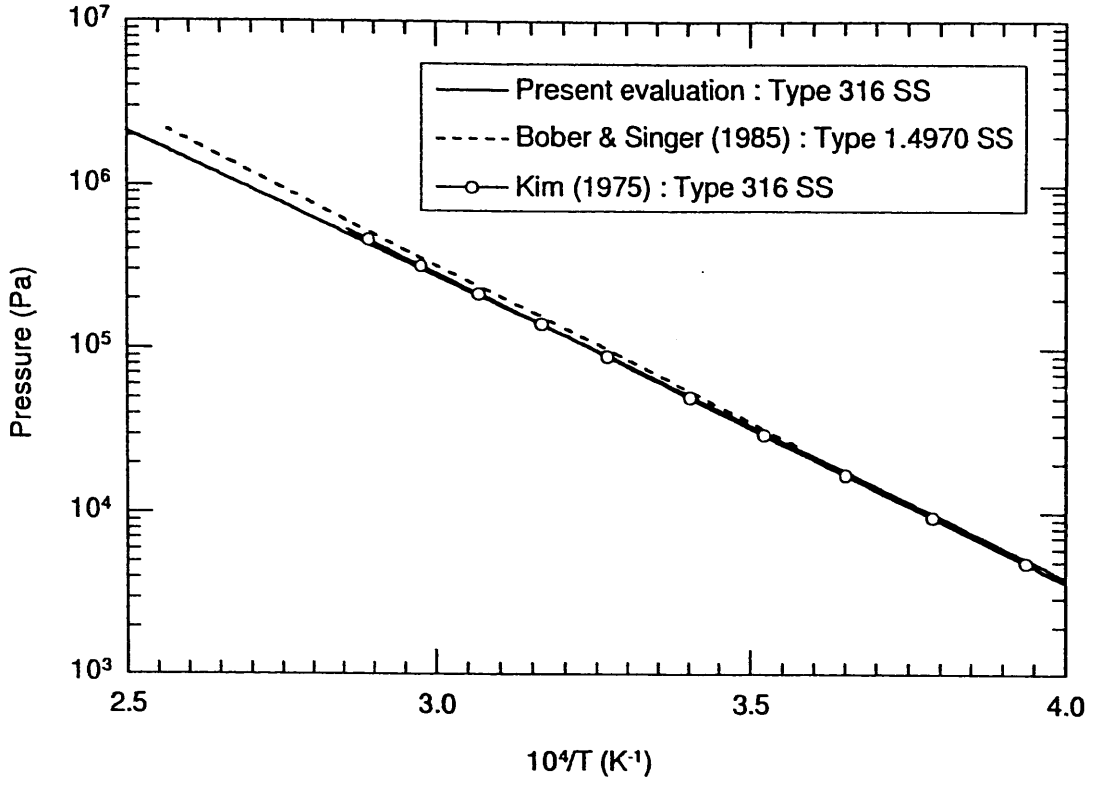


Fig. 1. Vapor pressure of stainless steel.

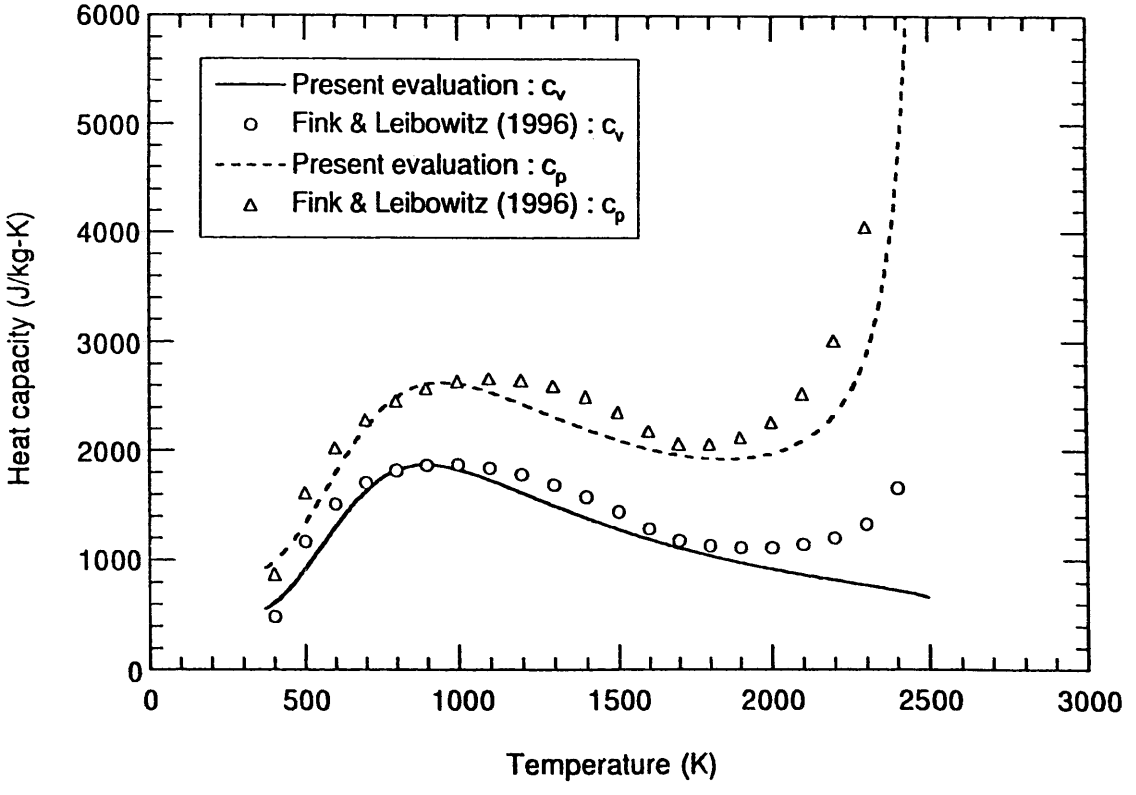


Fig. 2. Heat capacity of saturated sodium vapor.

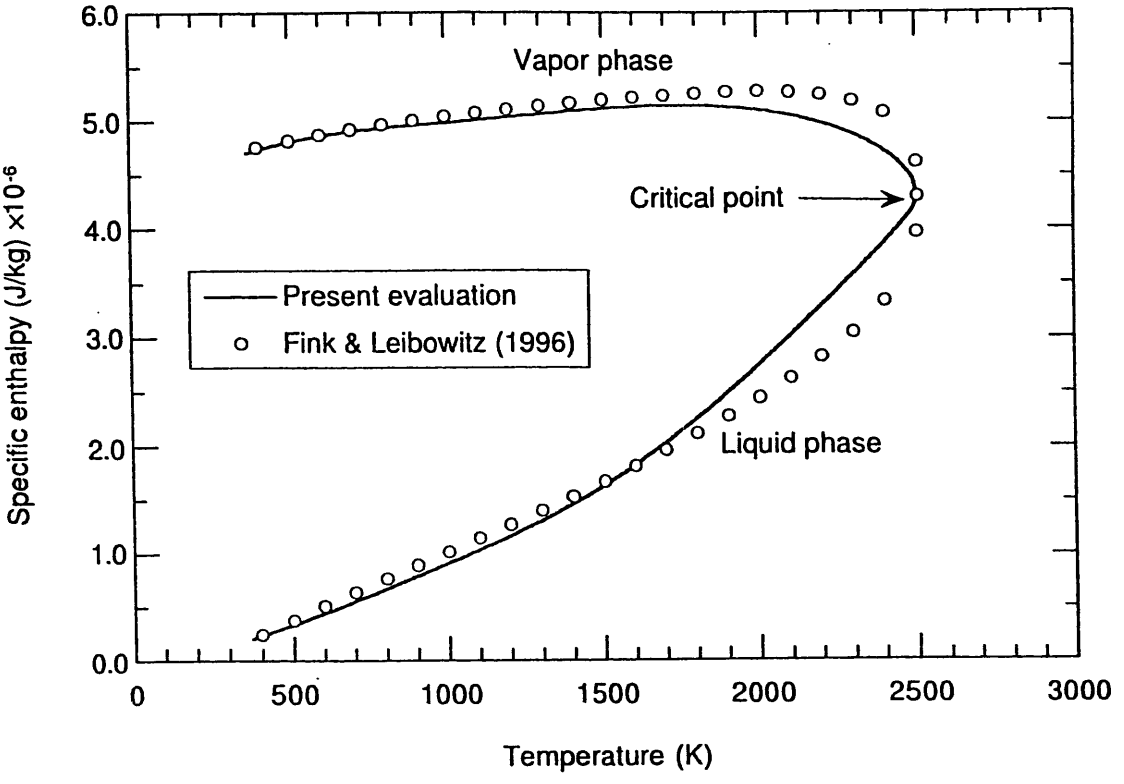


Fig. 3. Specific enthalpy of saturated sodium.

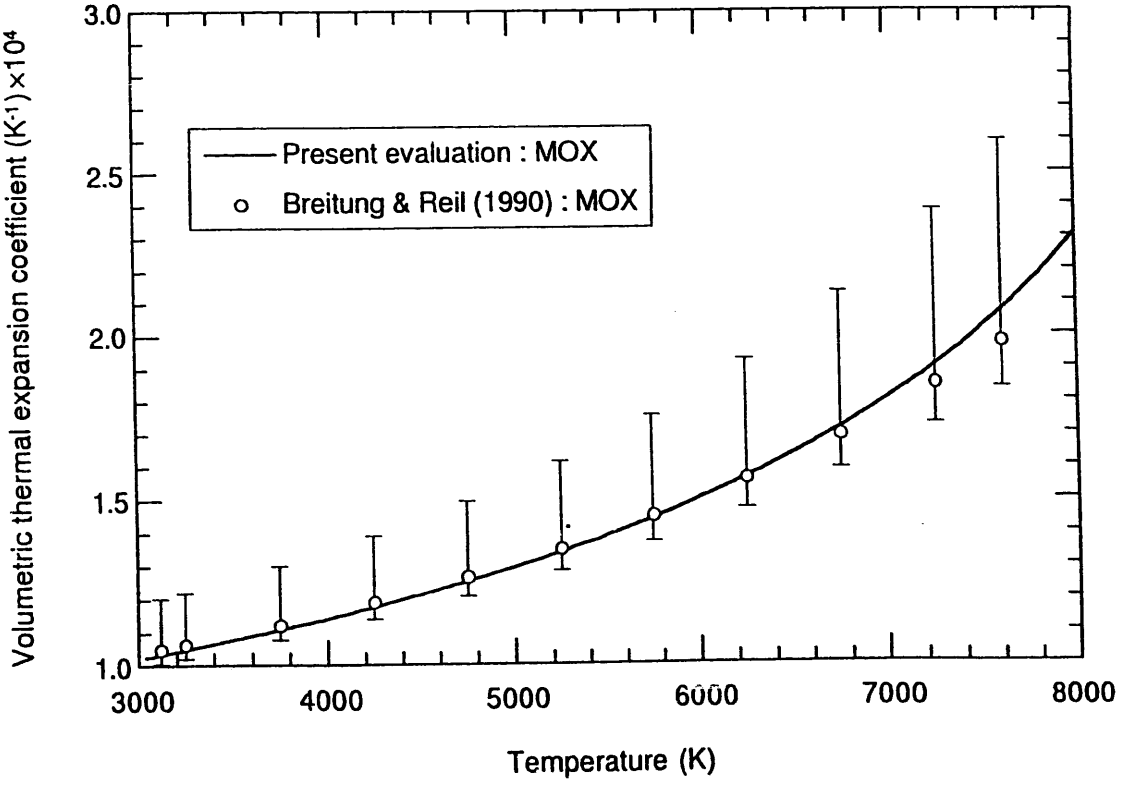


Fig. 4. Volumetric thermal expansion coefficient of liquid MOX.

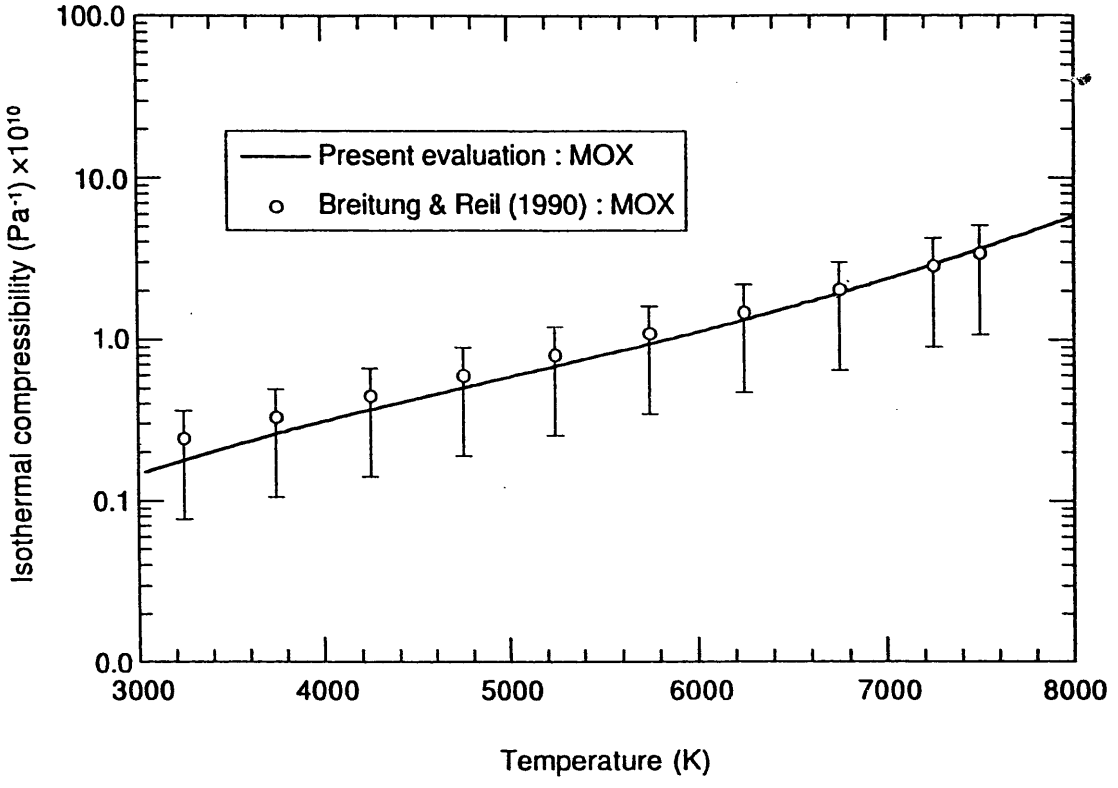


Fig. 5. Isothermal compressibility of liquid MOX.

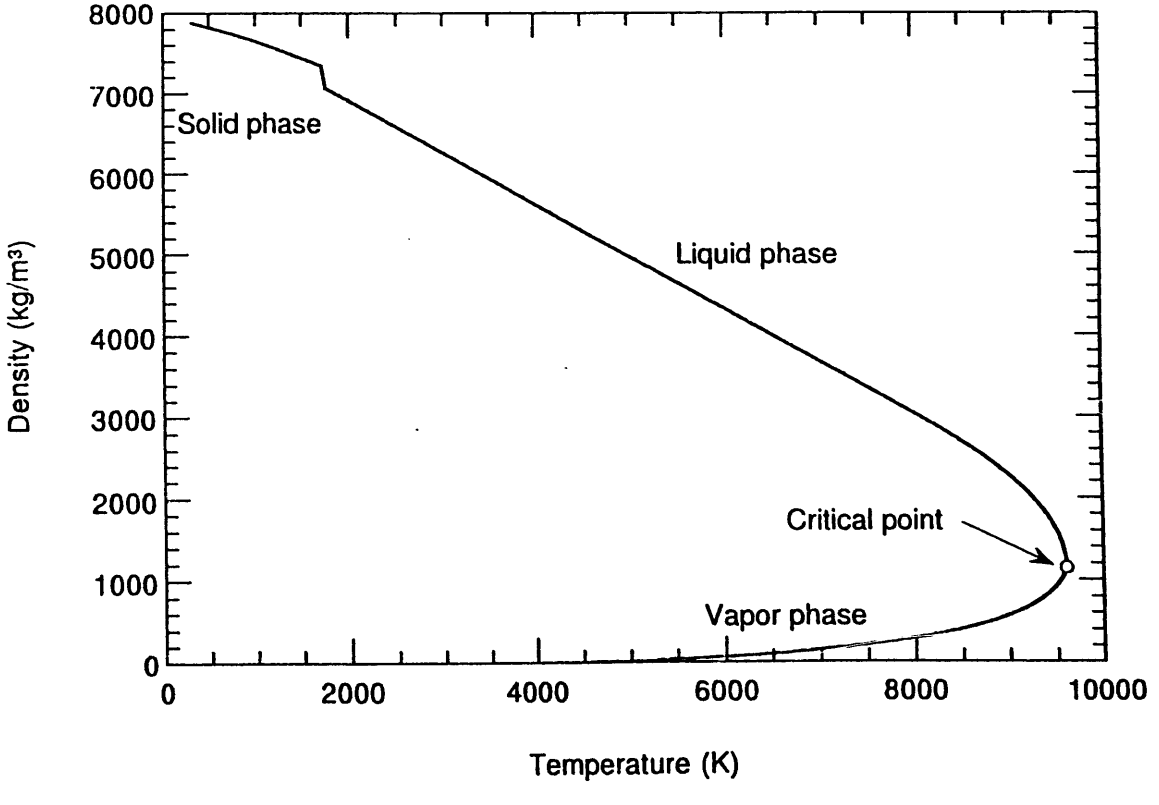


Fig. 6. Density of type 316 stainless steel on saturation curve.

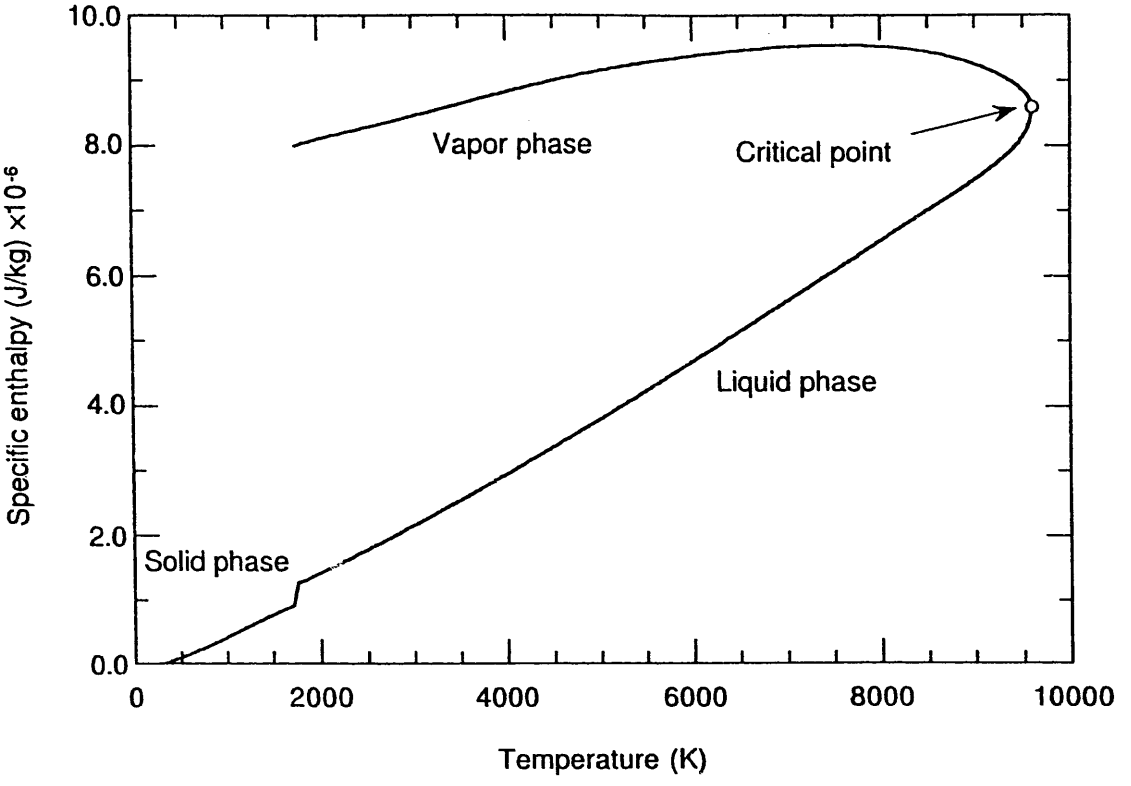


Fig. 7. Specific enthalpy of type 316 stainless steel on saturation curve.